




Case Study

An assessment on the inner lining need for a large-span tunnel (a case from Turkey, Akyazı Tunnel, Trabzon)

Ebu Bekir Aygar¹ · Candan Gokceoglu² 

Received: 2 January 2021 / Accepted: 11 February 2021 / Published online: 15 March 2021
© The Author(s) 2021 

Abstract

Stability of large underground structures depends on not only rock mass conditions but also excavation stages and support systems. In addition, complexity of geological conditions and interaction of excavation with in situ conditions affect the performance of design. The Akyazı tunnel (Trabzon, Turkey) is 2478 m long and was designed as 3 lanes and double tubes, and the number of lanes at the junction part increases to 5. Tunnel cross-sectional area from the Akyazı tunnel reaches 3 lanes and 150 m² to 5 lanes and 438 m² gradually. The width of the tunnel at the junction point reaches to 31 m. In this study, the necessity of inner lining concrete in tunnels excavated in good rock mass conditions is assessed and the results of the analyses are discussed. The inner lining concrete increases the cost of tunnel construction, as well as extending the construction period. With the procedure followed in the Akyazı tunnel, the top heading part of the tunnel was constructed without inner lining. No stability and drainage problem have not been encountered for 4 years. Currently, the tunnel construction was completed successfully, and the tunnel was opened to traffic. Consequently, the excavation stages, support systems described, and especially inner lining necessities discussed in this study may be applicable for extremely large tunnel sections.

Keywords Inner lining · Support system · Excavation · Akyazı tunnel · Large-span road tunnel

1 Introduction

The effective transportation is one of the basic requirements of sustainable developments, and one of the important components of effective transportation system of urban areas is tunnel. In tunnels with large underground openings, the most crucial problems encountered during excavation and support implementation are the stability of tunnel face and ceiling. When the developed methods are investigated, implementation of fiber bolts, wire mesh, and shotcrete is considered appropriate for the tunnel face. Also, for tunnel ceiling, application of fore poling method (implementation of umbrellas) is suitable to

ensure the stability of the ceiling by avoiding potential failures. In addition to all these supporting systems, the tunnel face excavation is divided into sections such as top heading, bench, and invert. If necessary, the top heading section can be divided into two or three sub-sections in the large-span underground openings. [1] and [2] and [3] investigated the problems and suggested various solutions. These studies elaborated tunnel face stability and the design of support system in squeezing and swelling ground conditions. Barla [4] examined the full-face tunneling in large tunnels under difficult conditions and stated that when the full section tunnel boring method is possible, existence of many advantages of that method

Supplementary information The online version contains supplementary material available at (<https://doi.org/10.1007/s42452-021-04366-1>).

✉ Candan Gokceoglu, cgokce@hacettepe.edu.tr | ¹Fugro Sial Geosciences Consulting Engineering Ltd, Ankara, Turkey. ²Department of Geological Engineering, Hacettepe University, Beytepe, Ankara, Turkey.



SN Applied Sciences (2021) 3:457 | <https://doi.org/10.1007/s42452-021-04366-1>

was also emphasized by different researchers. Sharifzadeh et al. [5] studied the method of excavation in large tunnels that were excavated in weak ground conditions. Jiao et al. [6] considered the steel tube slab (STS) method for subway stations with a very shallow overburden thickness and large underground openings, and they manifested both numerical analysis and applications methods relevant to this subject. Hoek [7] and Schubert [8] proposed a deformation slot and heavy steel shoring as solution suggestions. Aygar and Gokceoglu [9] analyzed the problems encountered during excavations of large railway tunnel, and they emphasized that the face stability is the most important factor for large tunnels constructed in shallow and weak ground conditions. One of the most important tunnel problems is squeezing, and Azizi et al. [10] studied on the squeezing conditions of rock mass encountered in the Kerman water conveyance tunnel. However, tunnel excavations in squeezing ground show large time-dependent and often anisotropic deformation [11]. An approach for the classification and prediction of large deformation in tunnel construction stage was recently proposed by Liu et al. [12]. Problems and possible measures in three-laned and double-tubed Bolu tunnels, whose construction is ongoing for a period of almost 20 years, are an example of large diameter tunnels [13] and [14]. As can be seen from short review, the researchers considered main support systems. However, Broch et al. [15] investigated the inner lining systems in the road tunnels opened in Norway. According to Broch et al. [15], the inner lining concrete is required for drainage and fire conditions. In addition, considering that the outer lining loses its bearing in the long term, the inner lining is considered to be an element that carries earthquake loads in the long term [15]. Wales and Lorenz [16] investigated the long-term behavior of support elements in tunnels excavated with conventional methods, and they stated that the bearing capacity of the outer lining does not decrease in the long term over 30 years. Consequently, according to the results of [16], there is no need for inner lining in the long term for the stability of tunnels excavated in good rock mass conditions. In addition, Grønhaug [17] described different methods for lining the tunnels in Norway, and the use of different methods of inner lining, such as lightweight structure, metal sheet linings, plastic sandwich linings, PE foam linings, tunnel fabric for protection from frost and for the drainage of water, was investigated. Additionally, Neuner et al. [18] stated that a single permanent shotcrete lining can fulfill the reduced requirements and offers a very economic tunnel design, in some cases, and they proposed a detailed finite element model for analyzing the bearing capacity of the permanent shotcrete lining on the basis of an advanced constitutive model considering

the time-dependent and nonlinear material behavior of shotcrete.

When considering these studies, it is evident that large-span tunnels and inner lining necessities are still not solved completely. For this reason, the purpose of the present study is to analyze the necessity of inner lining concrete in an extremely large tunnel excavated in good rock mass conditions. Within the context of the present study, the first-time application of a method in highway construction of Turkey, which is the expansion of the tunnel diameter by constructing a connection tunnel inside the tunnel, is also investigated. Numerical analysis methods for large diameter tunnel with an excavation diameter of 31 m are applied, and the experiences obtained from the study are presented.

2 Tunnel specifications

Trabzon is the most developed city of Black Sea region of Turkey, and the topography of Trabzon city is extremely steep. Due to steepness of topography, to find suitable sites for settlement and transportation is exceedingly difficult. Trabzon City Crossing Kanuni Boulevard Project is approximately 23 km long and comprises 9 tunnels within the scope of the project. The first tunnel of the project is the Akyazı tunnel whose left tube is situated between Km: 0+764–3+180 with a length of 2416 m, while right tube is situated between Km: 0+764–3+242 with a length of 2478 m (Fig. 1). The tunnels are designed as double tubes and three lanes. In the project route, the tunnel starts with an altitude of 9.07 m at Km: 0+762 and ends at an altitude of approximately 9.80 m at Km: 3+242 with an inclination of 0.64%. The Akyazı tunnel provides access to the newly built stadium and sport complexes as an alternative to the existing coastal road, while 616-m-long 2-laned connection tunnel is separated from the Akyazı tunnel to provide a connection to the boulevard. In the transition zone between the Akyazı tunnel and the connection tunnel, the cross section expands from 3 lanes and approximately 150 m² to 5 lanes and 438 m² (Fig. 1). The tunnel excavation was initiated in 2013, and it was completed successfully at the end of 2015.

The typical cross sections of the expansion region of the tunnel are given in Fig. 2a, b, and c. As can be seen from those sections, the tunnel diameter gradually increases from 16 to 31 m. This expansion was established in a 175 m distance inside the Akyazı tunnel. During the excavations, the expanding support applications were implemented, and each round length was limited to 50 cm. Expansion section is interesting for international tunnel community, and the analyses applied for this section are original. The

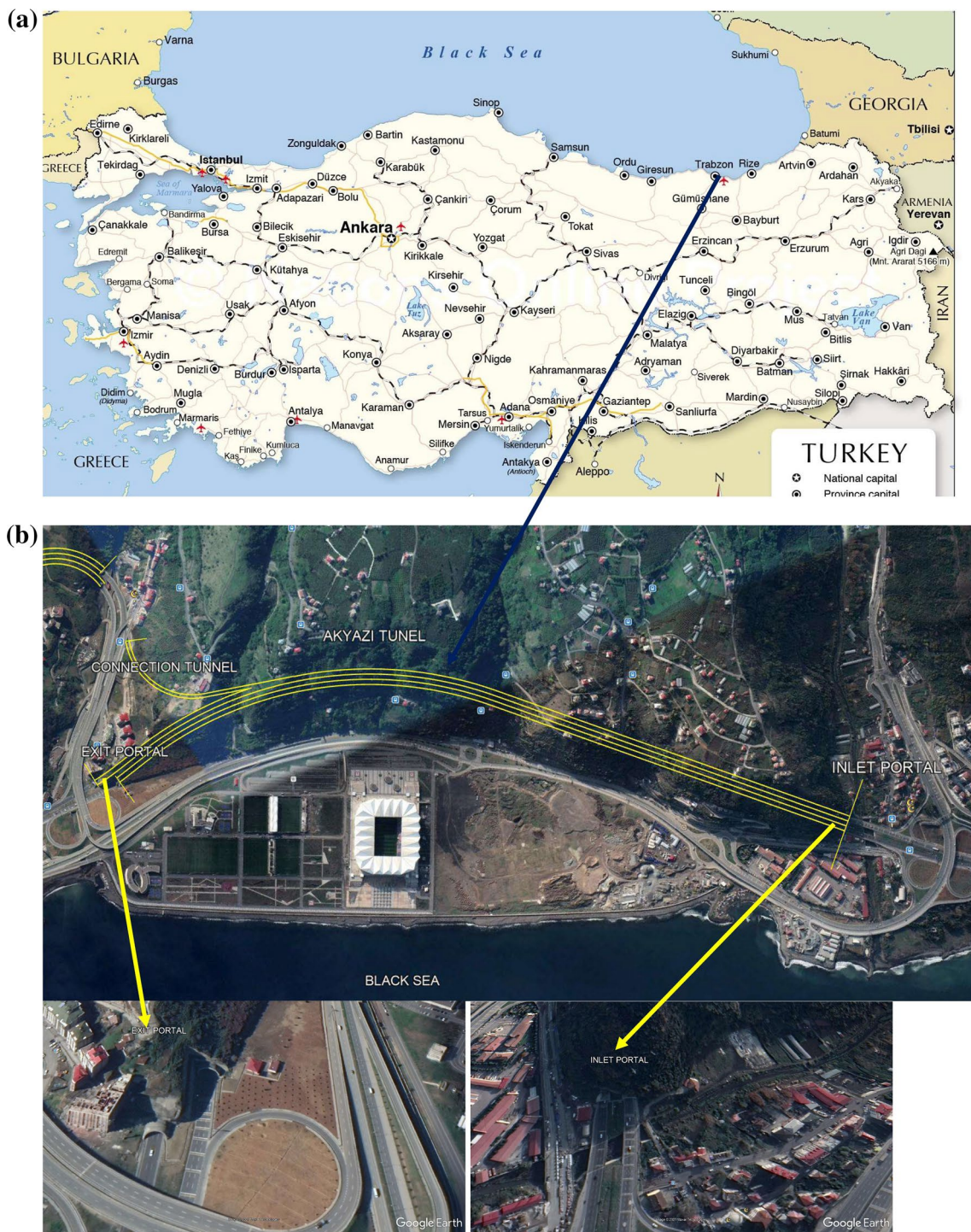


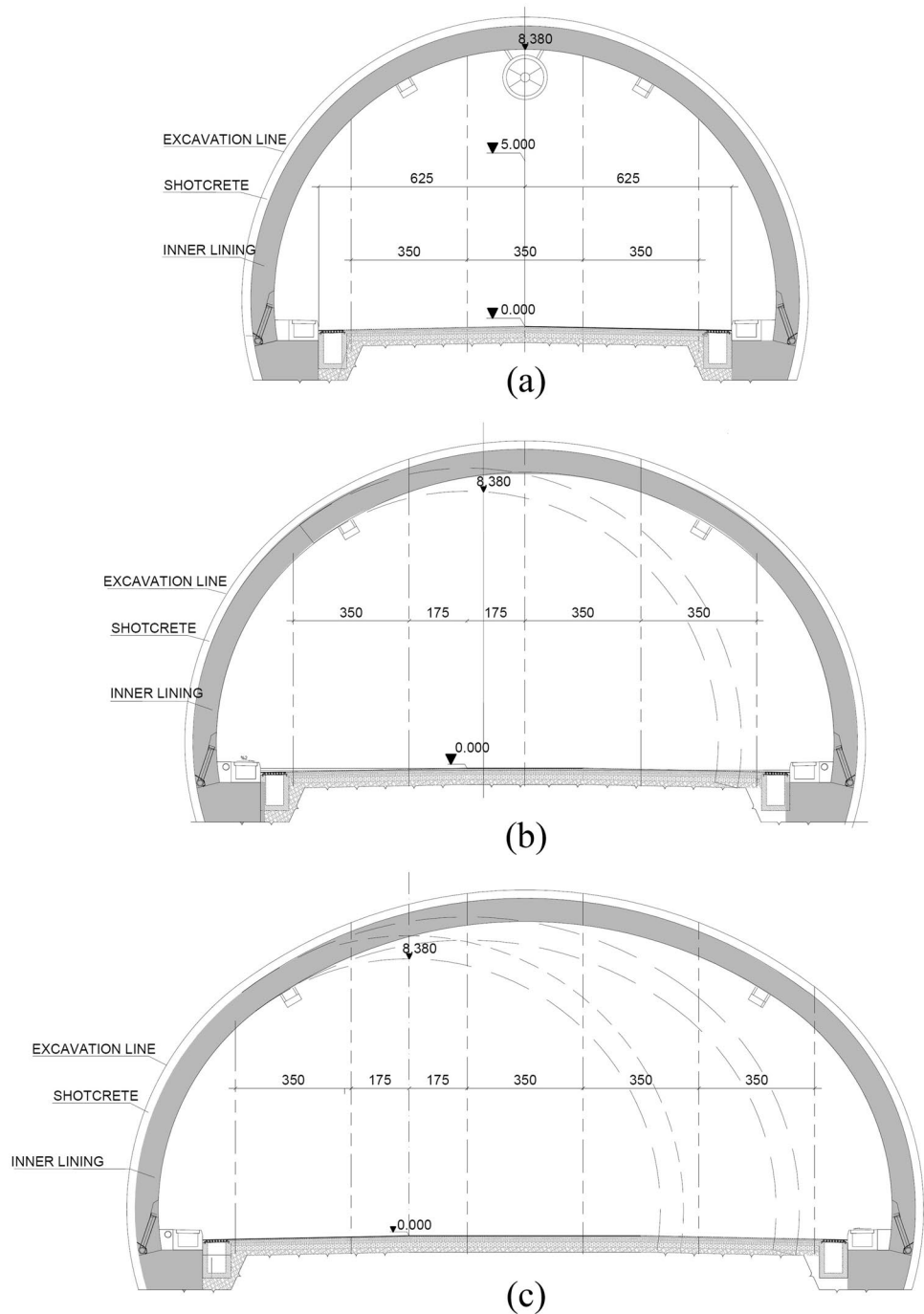
Fig. 1 **a** Location map; **b** expansion section

tunnel was excavated by blasting. Blasting parameters and environmental effects of blasting were studied by Ak and Aksoy [19].

3 Geological–geotechnical setting

Tunnel route completely passes through Pliocene aged Beşirli Formation [21] comprising coarse-grained gravel

Fig. 2 Typical cross sections of **a** expansion section-4 lanes; **b** expansion section-5 lanes; **c** the widest section (diameter is 31 m) [20]

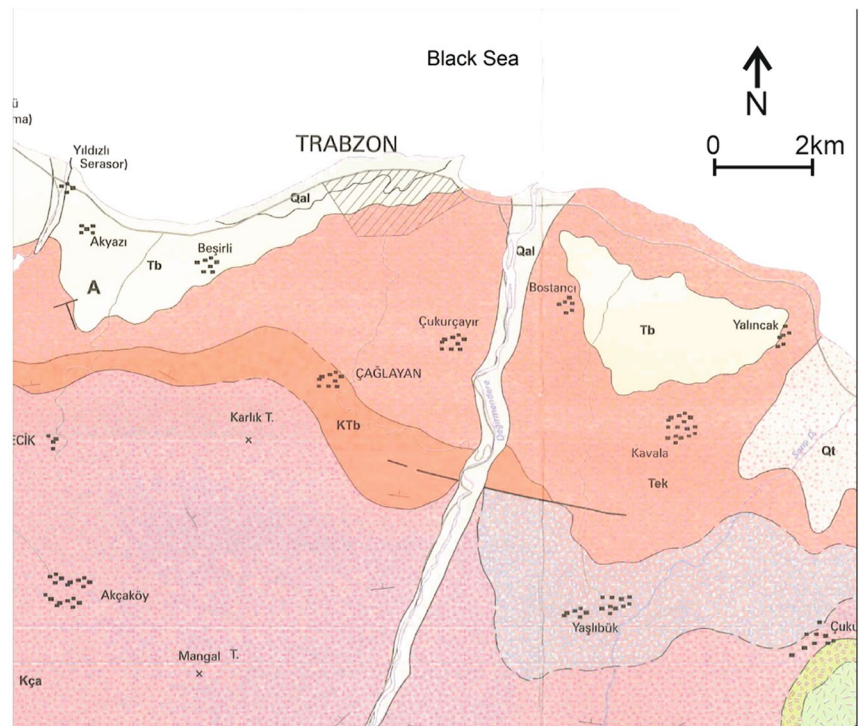


stone and sandstone with a thickness changing between 50 and 75 cm. The formation is generally composed of loosely cemented, coarse-grained agglomerate with local sandstone, claystone, and tuff interbedding. Agglomerate unit occasionally composed of coarse-grained andesite or basalt pebbles and blocks (Fig. 3 and Supplementary 1).

To examine the geological–geotechnical characteristics of the route through which Akyazi tunnel passes, geological mapping, boreholes, in situ and laboratory tests were

conducted by Fugro Sial [20]. For this purpose, total 9 boreholes were drilled with a total depth of 846 m in order to determine engineering characteristics and groundwater conditions along the tunnel route. Geological units, weathered zones, discontinuities, and possible weakness zones were identified by drilling and field studies along the route, and a geological cross section along the tunnel route was drawn. The entrance portal was excavated within the sand and clay layers of the Beşirli formation,

Fig. 3 Geological map of the tunnel route and its close vicinity [22]. Qal: Quaternary alluvium, Tb: Beşirli formation, Tek: Kabaköy formation, KTb: Bakırköy formation, KÇb: Çayırbağ formation, KÇa: Çağlayan formation



Qal : Quaternary alluvium
Tb : Beşirli formation
Tek : Kabaköy formation

KTb : Bakırköy formation
KÇb : Çayırbağ formation
KÇa : Çağlayan formation

while the exit portal was excavated through the sand unit of this formation. In the sandy levels, there are thin and poorly cemented zones. One (TSK-5) of the 9 boreholes is located in the expansion section of the tunnel (Fig. 4). This section constitutes a 250 m section between Km: 2+470–2+720. According to the outcrop observations during the geological mapping studies, the unit between Km: 2+470–2+720 was described as yellowish brown, moderately highly weathered, weak–medium strong agglomerate with a clast size ranging between 10 and 70 cm (Supplementary 2). Geotechnical parameters were assigned for the unit encountered by interpreting the data obtained from the borehole TSK-5 (Table 1) for this section.

The geotechnical design parameters for the gray-colored, fresh slightly weathered agglomerate between Km: 2+470 and Km: 2+720 were determined by the Hoek and Brown [23] failure criteria, and the values used for this purpose are GSI (geological strength index), UCS (the uniaxial compressive strength of the intact rock), and m_i (dimensionless material constant of the rock material) were obtained. The geological strength index (GSI) for the lithological unit along the expansion section was determined in accordance with the GSI system proposed

by Hoek and Marinos [24] (Fig. 5), taking into account the data obtained from the outcrops and borehole of TSK-5. For the range of Km: 2+470–2+720, the GSI value of the fresh slightly weathered agglomerate was determined as 45 (Fig. 5). Average value of uniaxial compressive strength of the specimens obtained from fresh slightly weathered agglomerate was found as 24 MPa. The modulus of elasticity of the agglomerate was determined as approximately 35 GPa. The material constant (m_i) is taken as 19 as suggested by Hoek and Brown [23].

The design parameters calculated for the fresh slightly weathered lithological unit are summarized in Table 2, and the failure envelope of Hoek and Brown (1980) criteria was obtained from the RocLab program (Fig. 6).

The modulus of deformation of rock masses is the most critical parameters when applying numerical analyses. For this reason, the dilatometer tests were applied in two boreholes (TSK 6 and 8) (Fugro Sial [22]). During the tests, the RocTest Probex Acculogix with 30 MPa radial capacity dilatometer was used. The modulus of deformation values varied between 3.9 GPa and 10.3 GPa. In total, 14 dilatometer tests were carried out in 2 boreholes, and Table 3 contains the summary of the dilatometer test results.

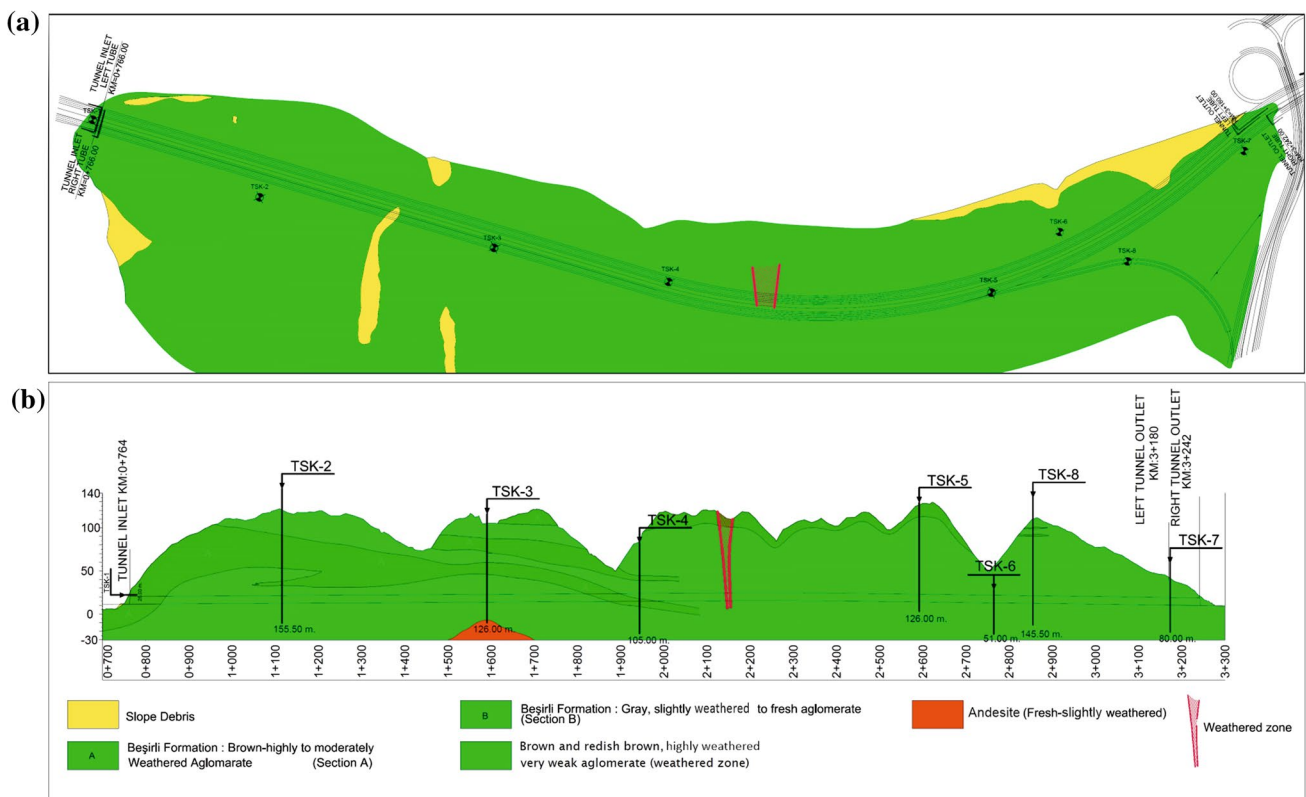


Fig. 4 a Geological plan and b geological cross section of the Akyazi tunnel [22]

The location of the project and its vicinity has low-earthquake hazard. Hence, the effective ground acceleration value (a_{max}) is specified as 0.1 g. According to TADB Research Engineering Services Technical Specification-2014, the horizontal earthquake acceleration used in the analysis is calculated as $a_0 = 0.05 \text{ g}$ ($a_{max}/2$) and the vertical ground acceleration value is calculated as 2/3 of a_0 , that is, 0.033 g [25]. In addition, it is recommended to reduce this value by 30% in tunnels with $h > 30 \text{ m}$ [26]. For this reason, it is seen that the earthquake hazard is not critical for the project.

4 Numerical analyses and deformation of tunnel support systems

Numerical analyses were performed using Phase2D v8.0 software. This software is a two-dimensional finite element program that models rock masses and their behavior under the effect of tunnel support systems. Underground excavations can be modeled in stages with the implementation of rock bolts, steel arches, wire meshes, and applications of shotcrete. Due to the existence of rock masses, material softening was assumed to be 60% for top

heading excavation and 40% for installation of support systems of top heading and bench excavation [27]. In addition, this ratio can be found by drawing the longitudinal deformation profile to determine the material softening in the tunnels. Here, the softening of the material can also be determined according to the maximum deformation rate of the deformation in the tunnel face. The longitudinal displacement profile can be drawn using the equation proposed by Vlachopoulos and Diederichs [28].

$$u = \begin{cases} u_{im} \cdot \left[\frac{\mu_{if}}{\mu_{im}} \cdot e^{x/r_0} \right] & , x < 0 \\ u_{im} \cdot \left[\frac{\mu_{im}}{3} \cdot e^{-0.15(r_{pm}/r_0)} \right] & , x = 0 \\ u_{im} \cdot \left[1 - \left(1 - \frac{u_{if}}{u_{im}} \right) \cdot e^{(-3x/r_0)/(2r_{pm}/r_0)} \right] & , x > 0 \end{cases}$$

where u_{if} deformation in the tunnel face. u_{im} : maximum displacement which occurs at r_{pm} scale.

The longitudinal displacement profile given in Fig. 7 is obtained from the equation of Vlachopoulos and Diederichs [28]. While the largest displacement occurs as 42 mm, it occurs as 12 mm in the excavation face, and 17 mm deformation occurs 1 m behind the excavation face.

Table 1 Laboratory test results [22]

Borehole	Specimen depth (m)	Unit weight γ (kN/m ³)	Uniaxial compressive strength UCS (MPa)	Modulus of elasticity E_i (GPa)	Poisson's ratio ν
TSK-5	57.00	57.20	2.25	15.60	0.42
TSK-5	76.50	76.75	2.28	23.80	0.45
TSK-5	116.50	116.85	2.43	37.50	0.34

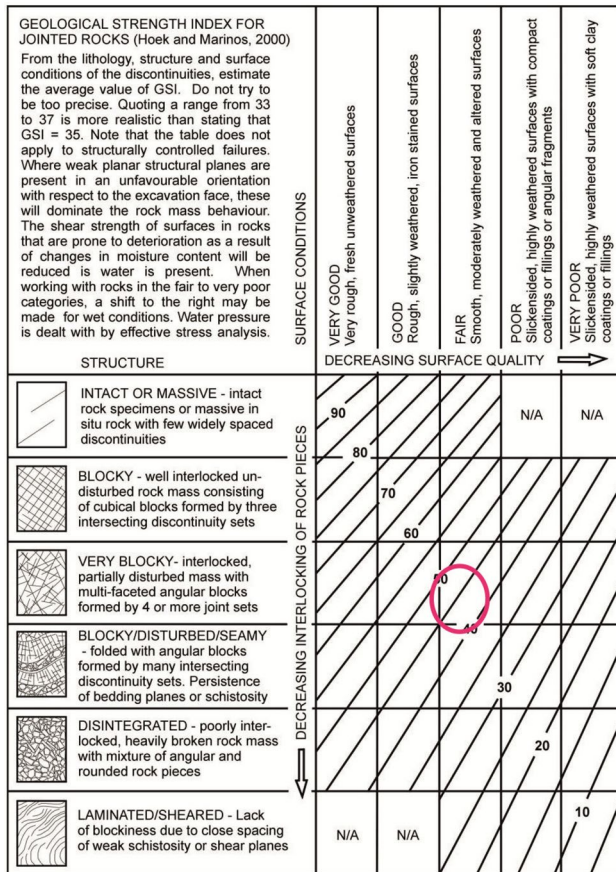


Fig. 5 Determination of the geological strength index (GSI) for the agglomerate unit between Km: 2 + 470—2 + 720 [24]

Table 2 Summary of geotechnical parameters for the fresh slightly weathered agglomerate along the expansion zone

UCS (MPa)	24
GSI	45
mi	19
D (disturbance factor)	0,7
Ei (GPa)	35
γ_n (kN/m ³)	24

In the numerical model, the Mohr–Coulomb failure criteria are employed, while boundary conditions are fixed in x and y directions, and constant field stress conditions are selected. In the expansion zone, the average

overburden is 100 m (Fig. 4), hence the vertical stress is calculated as ($\sigma_v = h \times \gamma$) 2.6 MPa, and the horizontal stress is obtained ($\sigma_h = k \times \sigma_v$) as 0.96 MPa. For the k value, the equation $k = 0.25 + 7E_m (0.001 + 1/z)$ given by Sheorey [29] is employed. The parameters used in this equation are as follows:

$$z = 103 \text{ m,}$$

$$E_m = 7.8 \text{ GPa.}$$

$$k = 0.83.$$

The model is generated 6-node triangles mesh. Two different cases were examined during the analyses. In the first case, the selected critical cross section where the diameter of the tunnel is 31 m, the analyses were separated into top heading and bench sections. The generated model of this section is given in Fig. 8.

In the second case, the tunnel was expanded in stages from 3 lanes to 31 m in dia., and the analysis was carried out. The model for this case is given in Fig. 9. This model was run in 23 stages. In this analysis, the deformations at the tunnel ceiling during expansion phase were investigated.

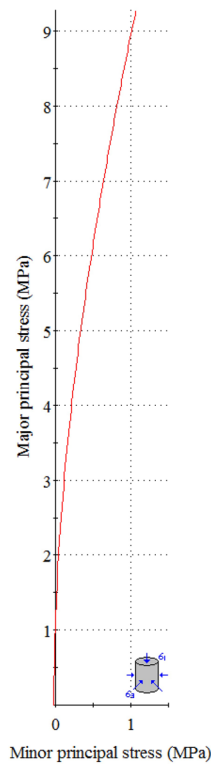
In this case, the excavation stages were considered step by step. In other words, the changes between the first excavation stage (D = 16 m) and the last excavation stage (D = 31 m) could be followed.

4.1 Evaluation of numerical analyses—first case

Top heading and bench sections of the largest zone of the tunnel were examined by numerical analyses. In the first case, the modeling steps for the right tunnel, after the application of tunnel support systems in the left tunnel, are given in Table 5 and in Figs. 10, 11, 12 and 13 that are some for stages.

When the results obtained from the analysis are interpreted, the total deformation and vertical deformation occurred in the right tunnel were under 1 cm (Figs. 14–15), and horizontal displacement is under 1 mm (Fig. 16). For the tunnel support systems, shotcrete lining (40 cm) with steel rib (HEB 200) is able to carry the load on them according to the support capacity plots given in Fig. 17. In addition, the axial force acting on the bolts is approximately 130 kN and the tensile strength of the bolts is 250 kN, and it is against the load (Fig. 18).

Fig. 6 Hoek–Brown failure envelope of the agglomerate



Hoek–Brown Classification

intact uniaxial comp. strength (σ_{ci}) = 24 MPa
 GSI = 45 m_i = 19 Disturbance factor (D) = 0
 intact modulus (Ei) = 35000 MPa

Hoek–Brown Criterion

m_b = 2.665 s = 0.0022 a = 0.508

Mohr–Coulomb Fit

cohesion = 0.424 MPa friction angle = 48.78 deg

Rock Mass Parameters

tensile strength = -0.020 MPa
 uniaxial compressive strength = 1.076 MPa
 global strength = 5.139 MPa
 deformation modulus = 7827.75 MPa

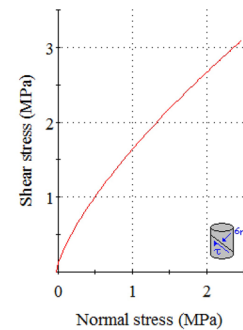


Table 3 Dilatometer test results [22]

No	Borehole No	Depth (m)	Em (MPa)
1	TSK-6	43,00	5190,725
2	TSK-6	45,00	3925,309
3	TSK-6	47,00	844,8149
4	TSK-8	70,00	7361,789
5	TSK-8	75,00	4802,408
6	TSK-8	80,00	3905,52
7	TSK-8	85,00	9642,961
8	TSK-8	90,00	10,491,77
9	TSK-8	95,00	5896,68
10	TSK-8	100,00	4238,059
11	TSK-8	105,00	7168,424
12	TSK-8	110,00	4350,717
13	TSK-8	115,00	10,284,86
14	TSK-8	120,00	8573,621

4.2 Evaluation of numerical analyses—second case

The modeling stages for the second case are presented in Table 6 for the right tunnel. Figures 19, 20, 21 and 22 show some modeling stages.

The modeling stages applied for the top heading section were also applied for the bench section, and eventually modeling stage was completed. In order to investigate the deformations emerging in each expansion during the

right tunnel excavation, analyses were performed for 4 different points on the right tunnel ceiling, and they are presented in Table 7 and Figs. 23, 24, 25 and 26. In the graphs, the deformations after each excavation stage at the specific points were examined. As can be seen from the analyses results, the maximum deformation in the tunnel is about 7.5 mm. When the rise in the deformation values was considered, it is clearly seen that deformations at point 1 were increased by 6.5 mm from the beginning of expansion till it was completed (Fig. 27), and in turn top heading was stabilized with the completion of the expansion. However, bench excavations were not affected by the deformations in the tunnel.

When the deformations at point 2 were considered, an increase in the deformations was identified with the start of the expansion excavation in mm scale. The values rose from 3.0 to 7.15 mm by the end of the expansion. The deformations at point 3 reached up to 7.8 mm by the end of the expansion excavation, while it was observed as 4.9 mm throughout the excavations works. This represents an increase of 7.8 mm which was the largest part of the tunnel. When the deformations calculated at point 4 were examined, 0.4 mm deformations occurred during the tunnel expansion excavation, and this value increased to 5.2 mm when the expansion phase was completed. For the tunnel support systems, it was clearly identified that steel reinforcements and shotcrete linings were able to carry the load on them according to the support capacity

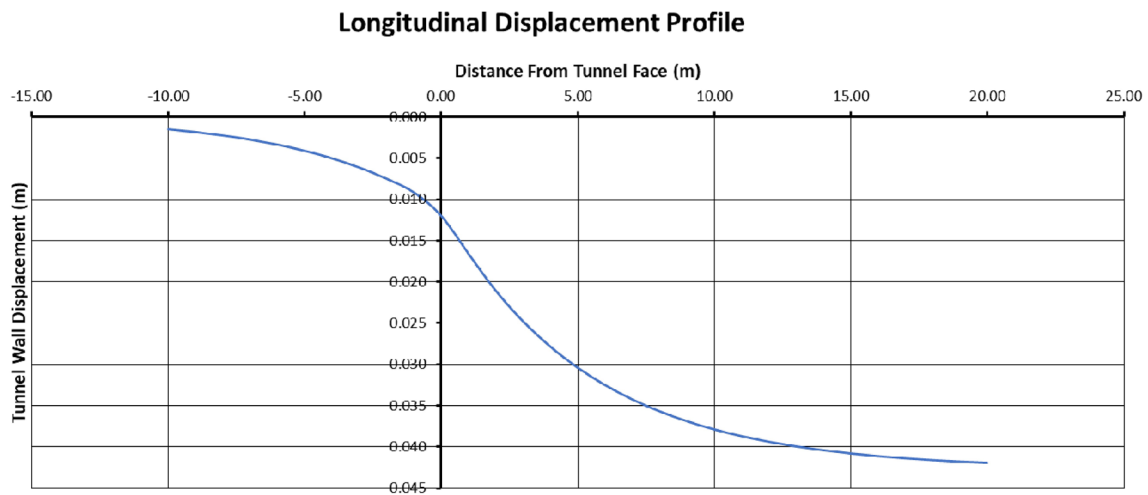


Fig. 7 Longitudinal deformation profile employing the relation proposed by Vlachopoulos and Diederichs [28]

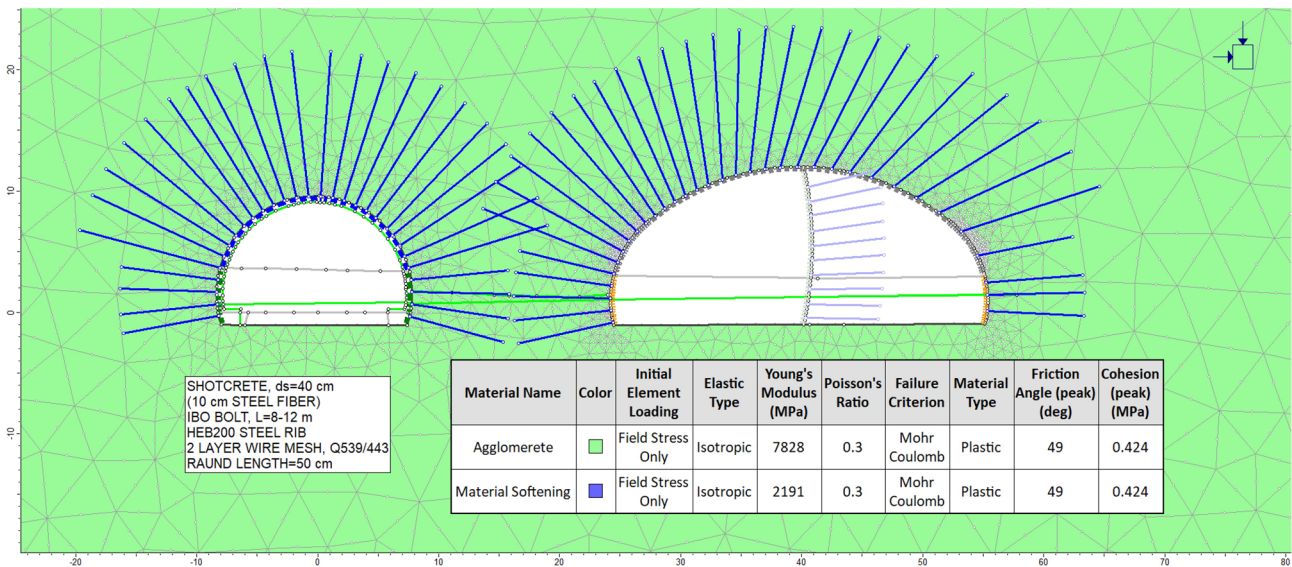


Fig. 8 Numerical model generated for the section with 31 m diameter

plots given in Fig. 28. Moreover, the axial force acting to the bolts is approximately 166 kN (Fig. 29). The ultimate strength of the bolts is 250 kN; hence, it is against the load. The deformations calculated are summarized in Table 7. When the deformation measurements were interpreted, it was determined that there would be no stability problems in the tunnel regarding to the tunnel support systems. Moreover, no problems were encountered throughout the excavation works.

4.3 In situ deformation measurements

To control the excavations and to compare the deformations obtained from the numerical analyses, the deformations were measured at Km: 2 + 544–2 + 569. In the convergence measurements, only 9 mm deformation occurred at Km: 2 + 544 over a period of approximately 4 months. The in situ measurement points are shown in Fig. 30. Here, the differences between the tunnel ceiling point and the left and right lower half points are examined. Measurements were made with a tape extensometer, and the differences in convergence between two points are shown. The points were measured every day immediately after the

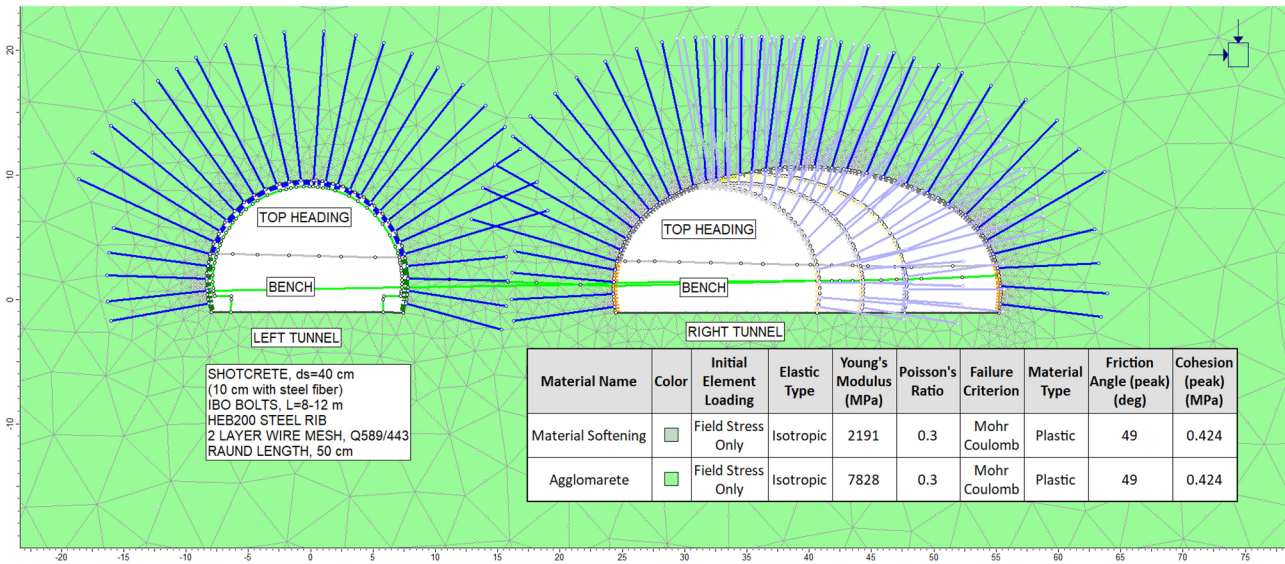


Fig. 9 Numerical model created for the expansion case during tunnel excavation

Table 5 Modeling stages of numerical analyses for the first case

Tunnel	Stage	Excavation stages
Left tunnel	1	Initial conditions
	2	Top heading excavation, material softening
	3	TH support installation
	4	Bench excavation, material softening
	5	Bench support installation
Right tunnel	6	Top heading (first section) excavation (material softening)
	7	Top heading (first section) support installation
	8	Bench (first section) excavation (material softening)
	9	Bench (first section) support installation
	10	Top heading (second section) excavation (material softening)
	11	Top heading (second section) support installation
	12	Bench second section excavation (material softening)
	13	Bench second section, support installation
	14	All support shotcrete hard
	15	Seismic loading

excavation, and then every 3 days, and then once a week until the deformations are complete.

In the measurement results at Km: 2 + 544, the deformations remained at the mm level from the beginning of the excavation, the largest displacement occurred is under 9 mm, after all, deformations were measured below 2 mm per month, and no deformation was observed thereafter (Fig. 31a). The measurement measurements at Km: 2 + 569 are given in Fig. 31b. As can be seen from Fig. 31b, deformations were measured at the level of mm and no deformation was observed afterward. There is a good agreement between the deformation values obtained from the numerical analyses and in situ measurements. In other

words, the maximum deformation values obtained from both numerical analyses and in situ measurements are under cm level.

4.4 Sequence of tunnel excavation and tunnel support application

In this stage of the tunnel construction, excavation and support operations have been completed primarily in the left tube and connection tunnel. After this stage, excavation and support operations were started in the right tunnel expansion zone.

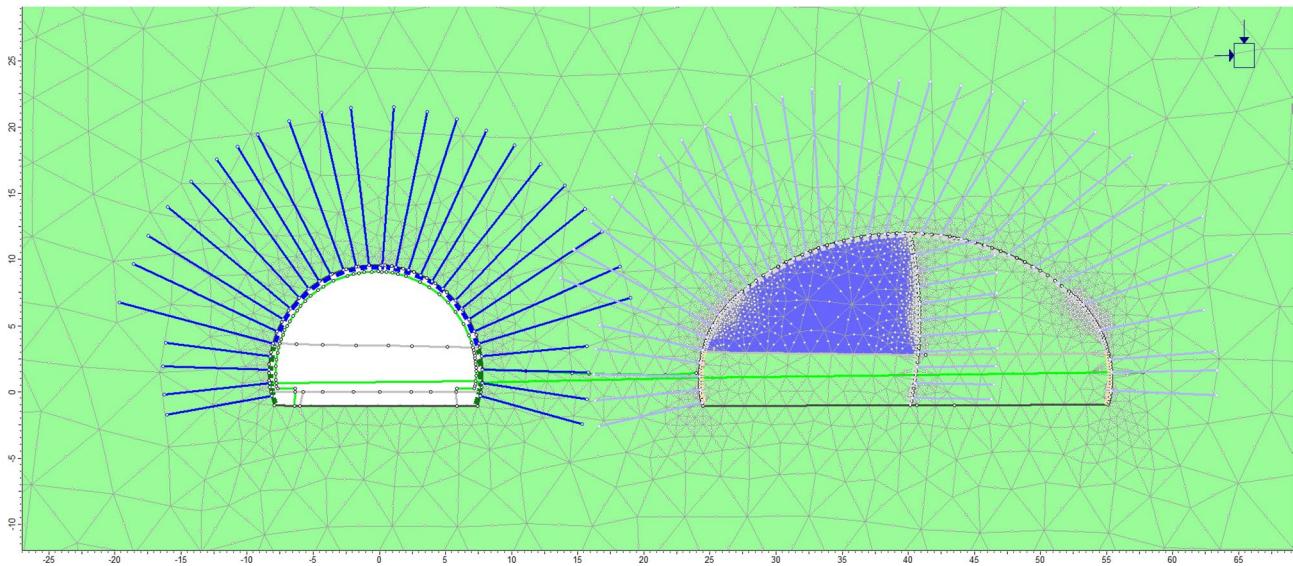


Fig. 10 Excavation of top heading first section of right tunnel; stage 6 in Table 5

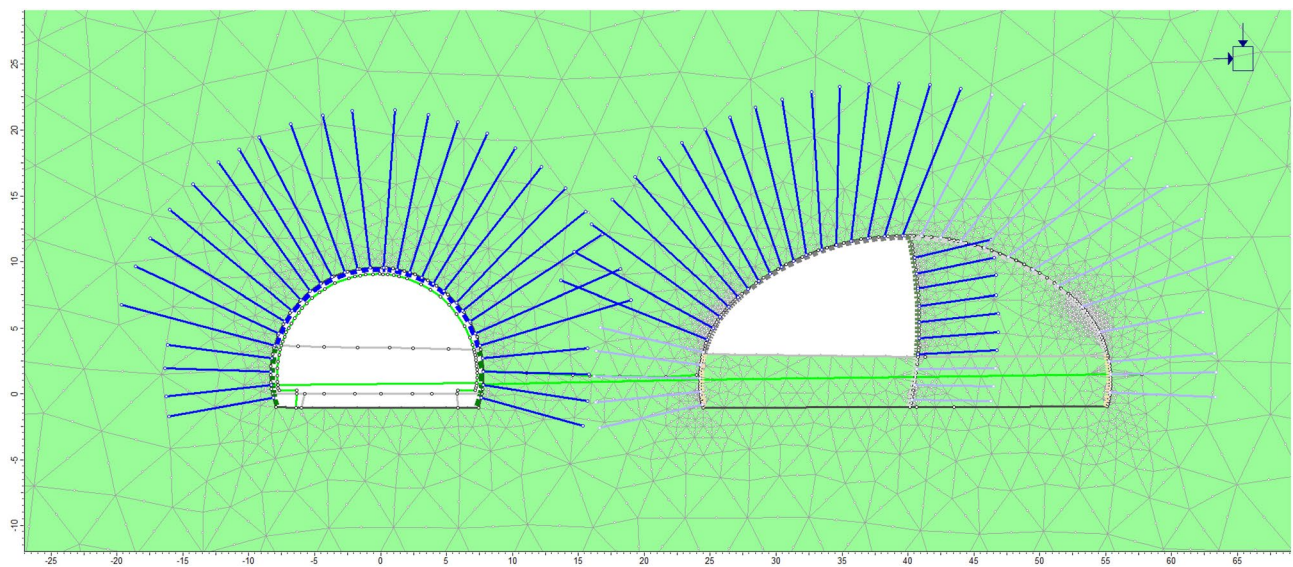


Fig. 11 Top heading first section of right tunnel support installation; stage 7 in Table 5

First, the top heading excavation was carried out in one stage between the beginning of the expansion and between Km: 0 + 000–0 + 063.98 (Fig. 32). Round lengths are limited to 50 cm (Fig. 33 and Supplementary 3–8).

During the excavation works, the left half of top heading was excavated at first by advancing 25 m (Stage 1), and then excavation at bench section was initiated (stage 2). After the excavation at left half of top heading and bench was advanced by 50 m with 25-m intervals, excavations at

right half of top heading were initiated (stage 3). After the excavation at right half of top heading was advanced by 25 m, excavation at right half of bench section was initiated (stage 4). A distance of 50 m was left between the excavations at left half of top heading and right half of top heading (Fig. 34).

As shown in Fig. 35, stage 1 excavation was carried out in the top heading by progressing 20 m, and stage 2 excavations were started at the bench section. All round

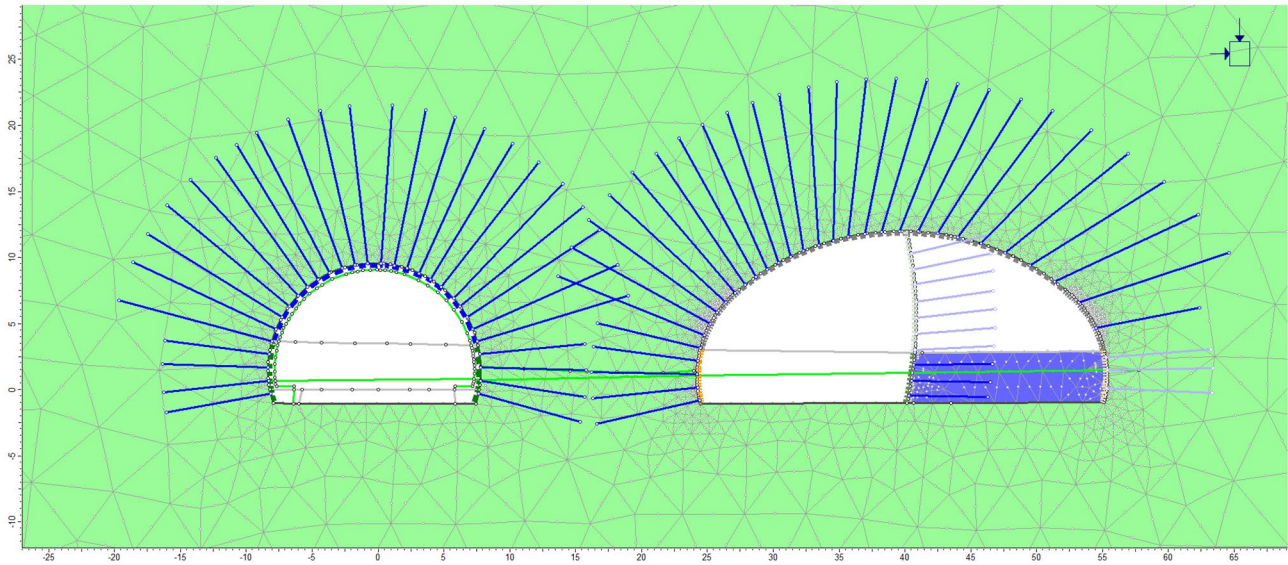


Fig. 12 Bench excavation for second section of right tunnel; stage 12 in Table 5

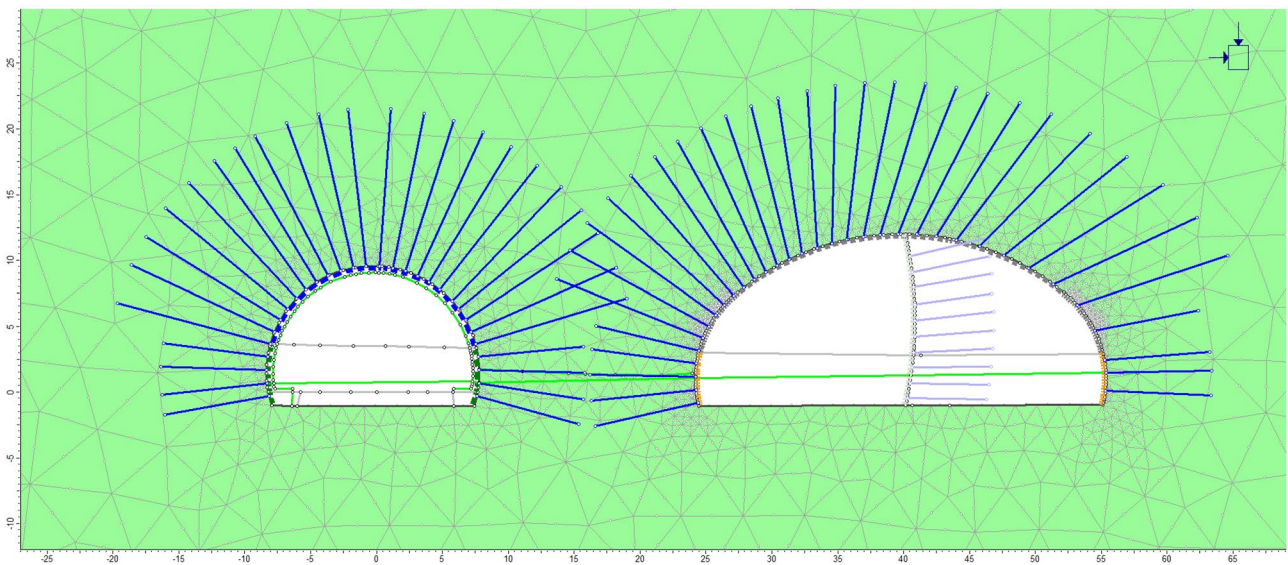


Fig. 13 Bench support installation for second section of right tunnel; stage 13 in Table 5

lengths were limited to 50 cm at the expansion section. After the completion of the first- and second-stage excavations in the tunnel, by setting off the third-stage excavations tunnel expansion was initiated. By determining specific reinforcements for each stage of excavation, application of tunnel support systems was progressed. Stage 4 excavations were initiated subsequently after finalizing stage 3 excavations (Supplementary 9).

4.5 Inner lining concrete construction

After the completion of the excavations and the installation of the support systems, it was understood that the stability was achieved in a short time in the expansion zone due to negligible low deformations. However, as the expansion zone gradually widened, a standard opening was not formed throughout the zone. In other words, the inner lining to be made in this part of the tunnel should expand both horizontally and vertically. For this reason, it is impossible with a mold that expands both horizontally

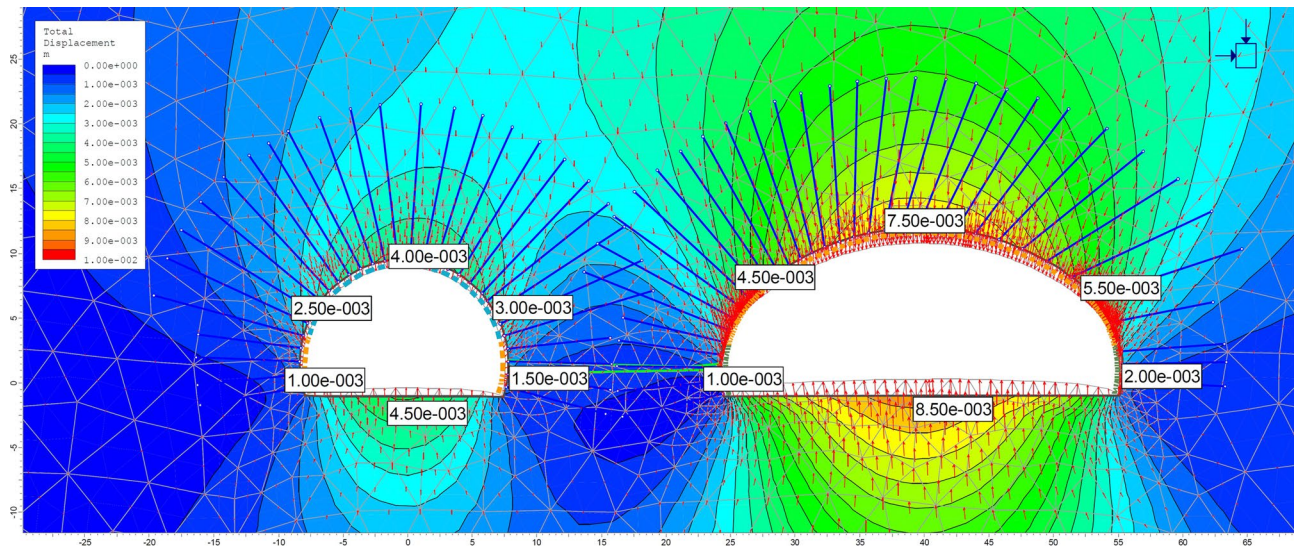


Fig. 14 Total displacements

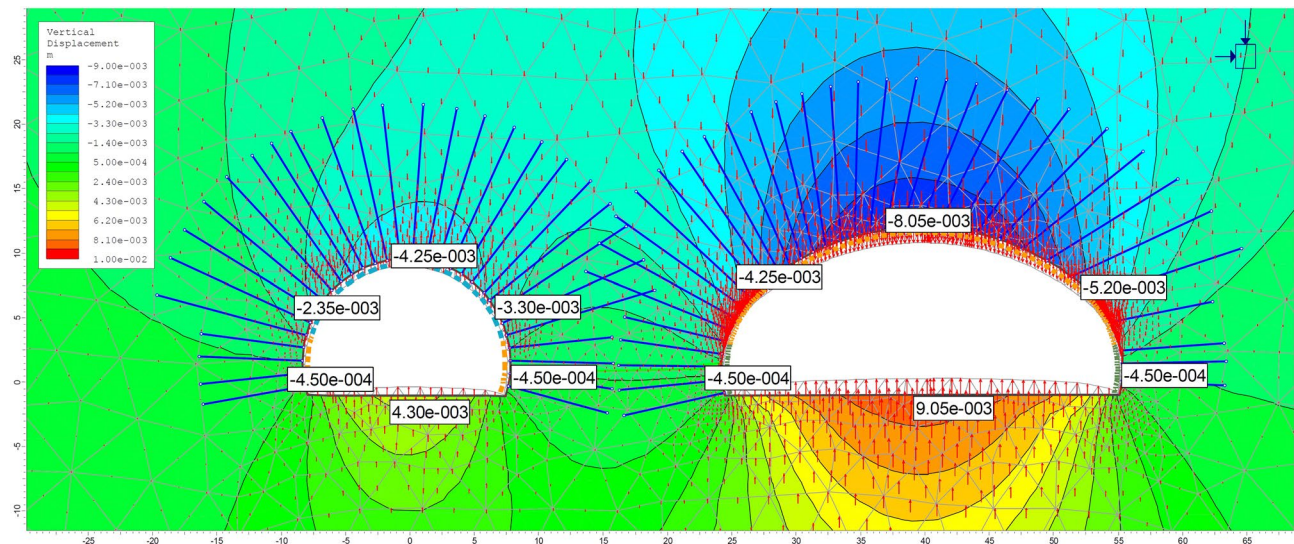


Fig. 15 Vertical displacements

and vertically with existing mold systems. Due to all these limitations, it has become impossible to make a standard concrete inner lining in the expansion zone of the tunnel. Owing to these reasons, special inner lining design was projected and applied in the expanding zone. In addition, it is questioned whether it is necessary for the inner lining concrete in tunnels, since it is not considered as a bearing element, especially in high-quality rock masses, and because it is made for the purpose of giving the tunnel architectural appearance and drainage. Instead of inner lining in tunnels excavated in good-quality rock masses, Broch et al. [15] and Grønhaug [17] suggested different alternatives. However, it is accepted that the outer lining loses its bearing capacity in long-term corrosion and

environmental effects. In addition, Lunardi [30] stated the problems encountered in large-scale tunnels, their solution suggestions and their suggestions for the full section tunnel boring method. However, the diameter of tunnel to be excavated by TBM must be constant. However, Galler and Lorenz [16] stated that the outer lining also continued as a bearing element for at least 30–40 years. For this reason, more economical solutions can be made instead of inner lining concrete, which causes serious amounts of cost. As Duffat [31] points out in his work, underground structures must be built with nature, not against it. Due to the fact that the expansion section of the Akyazi tunnel was excavated in good-quality rock mass, the inner lining concrete ceiling section was not projected. Therefore, a

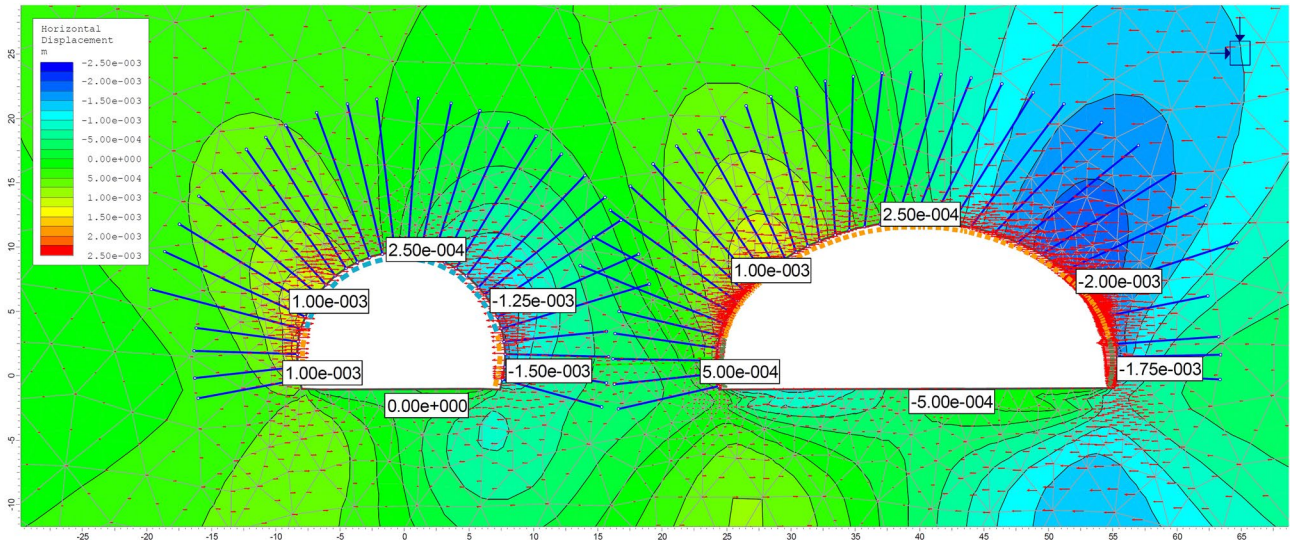


Fig. 16 Horizontal displacements

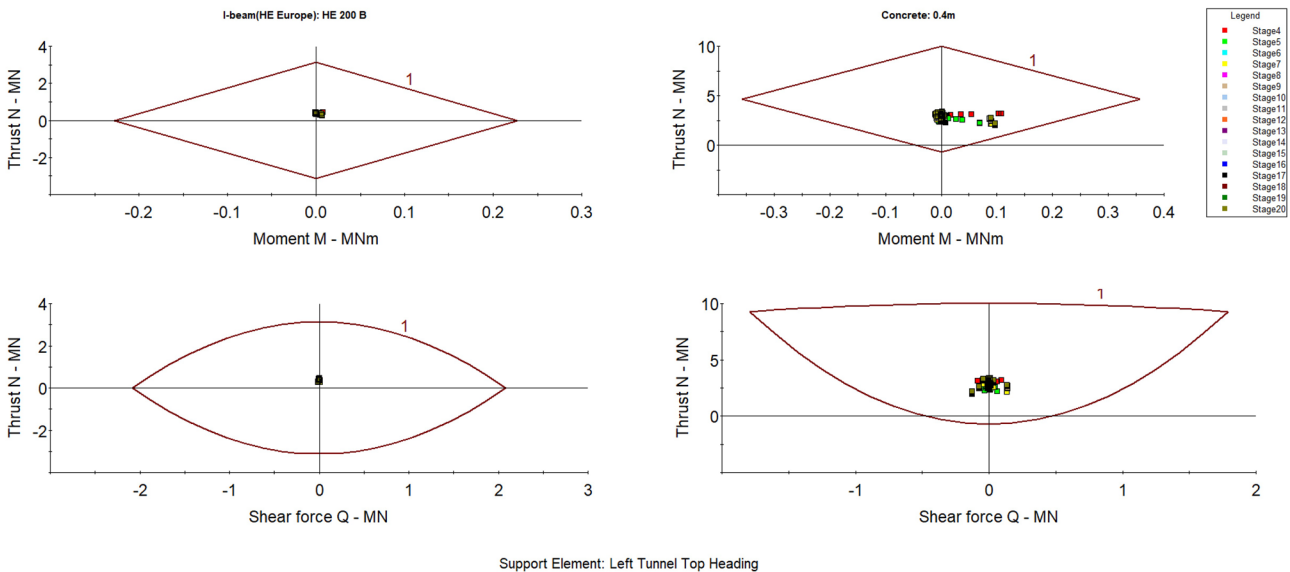


Fig. 17 Support capacity plots for first case

special lining system was needed for the expanded section of the tunnel (Fig. 35 and Supplementary 10–11). In this lining system, a membrane was laid primarily for the drainage of groundwater. Later, 70-cm-thick reinforced concrete structure was constructed exactly until +6.019 level. The reinforced concrete structure was fixed to the ground with 6-m-long anchors. It was covered with 10 × 60 × 120 Rockwool Jacketing Plate (40 kg/m³) for the cut in the tunnel ceiling starting from +6.019 level. Then tunnel ceiling lining was made with steel profiles.

With the proposed support systems, excavation works were completed without any instability problems inside

the tunnel. Supplementary 11–13 show the finished state of the tunnel. Finally, no problem has been encountered in the tunnel opened to traffic for 4 years.

5 Conclusions

In the study, the detailed analyses and a methodology for an extremely large road tunnel were presented and the necessity of the inner lining system was discussed, especially. In addition, all stages of the tunnel construction were observed and measured, and the performance of

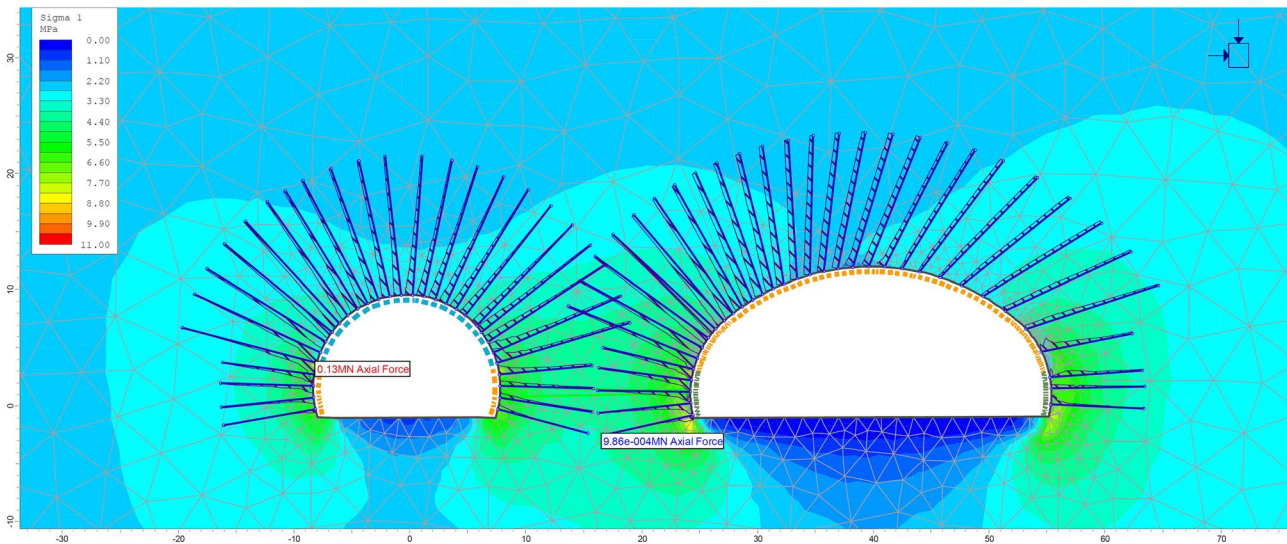


Fig. 18 Axial force at bolts for first case

Table 6 Modeling stages of numerical analyses for the second case

Tunnel	Stage	Excavation stages
Left tunnel	1	Initial conditions
	2	Top heading excavation, material softening
	3	TH support installation
	4	Bench excavation, material softening
	5	Bench support installation
Right tunnel	6	Top heading excavation, material softening
	7	TH support installation
	8	TH enlargement 1 excavation
	9	TH enlargement 1 support installation
	10	TH enlargement 2 excavation
	11	TH enlargement 2 support installation
	12	TH enlargement 3 excavation
	13	TH enlargement 3 support installation
	14	Bench excavation, material softening
	15	Bench support installation
	16	Bench enlargement 1 excavation
	17	Bench enlargement 1 support installation
	18	Bench enlargement 2 excavation
	19	Bench enlargement 2 support installation
	20	Bench enlargement 3 excavation
	21	Bench enlargement 3 support installation
	22	All support shotcrete hard
	23	Seismic loading

the proposed support systems was evaluated. Hence, the conclusions obtained from the study are drawn as follows:

The cross-sectional area of the enlargement part of the Akyazi tunnel reaches up to 438 m².

According to the results obtained by the analysis and by the experiences during construction phase, it is found that the most appropriate method is to apply partial excavation.

Since inner lining concrete does not have a load-bearing feature in good-quality rock masses, more economical methods should be chosen. Thus, serious economical benefits can be obtained in long tunnels.

When evaluating the need for inner lining for wide-span and long tunnels, the strength of the outer lining should be considered. Without inner lining, outer lining should not only serve as bearing element, but also play a role in waterproofing, fireproofing, and preventing cracks.

In such transition zones, considering that a possible collapse causes great problems, excavation and support operations should be undoubtedly executed by staying on the safe side. It is obvious that there is a requirement of rigid support system that would not allow any deformation during excavation stages. It is seen that deformation measurements obtained by analyses and values measured during construction are compatible with each other.

After the tunnel excavation, the first layer of shotcrete is critically important since it prevents possible loosening and cuts the ground's contact with atmospheric conditions. Besides, it is necessary to reinforce this shotcrete with wire mesh.

Consequently, there is a great consistency between the results of the numerical analyses and deformation measurements. Basically, the correct determination of rock mass parameters and local geological conditions led to consistent results from the numerical analyses. Local geological conditions and accurate determination of rock mass characteristic are the most important components of tunnel

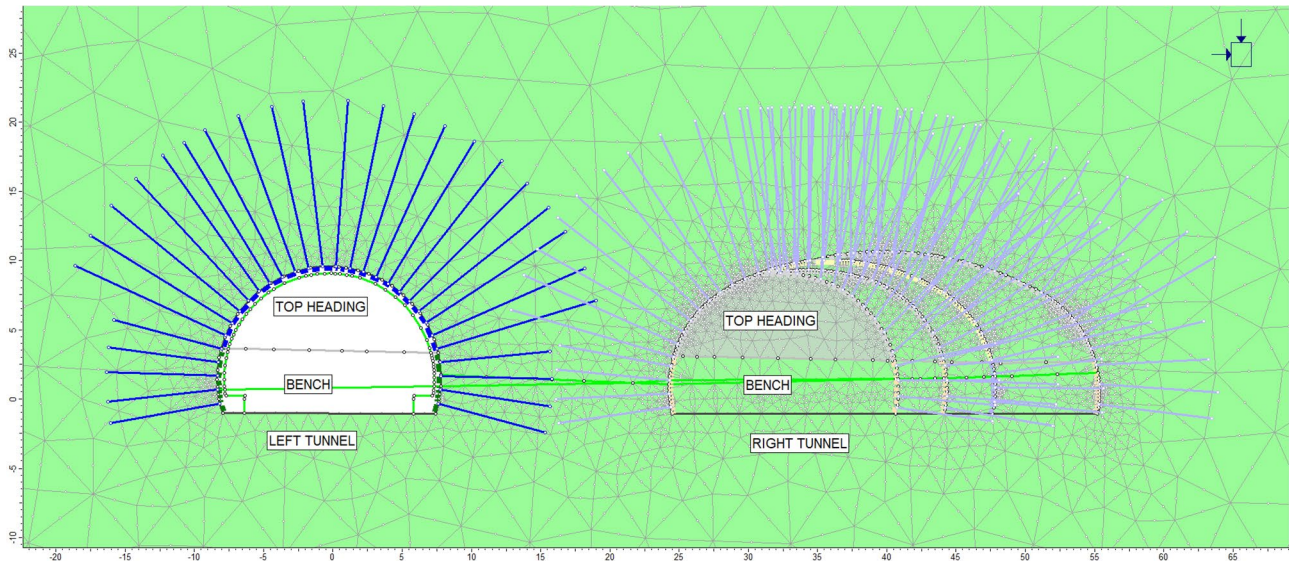


Fig. 19 Right tunnel excavation

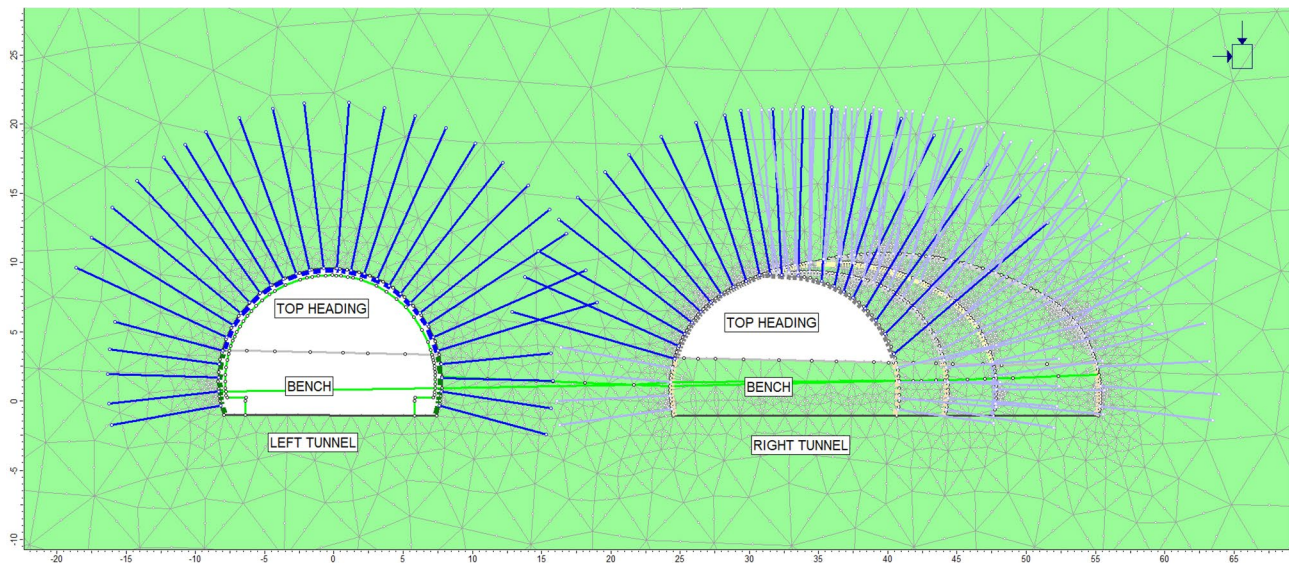


Fig. 20 Installation of tunnel support systems for right tunnel

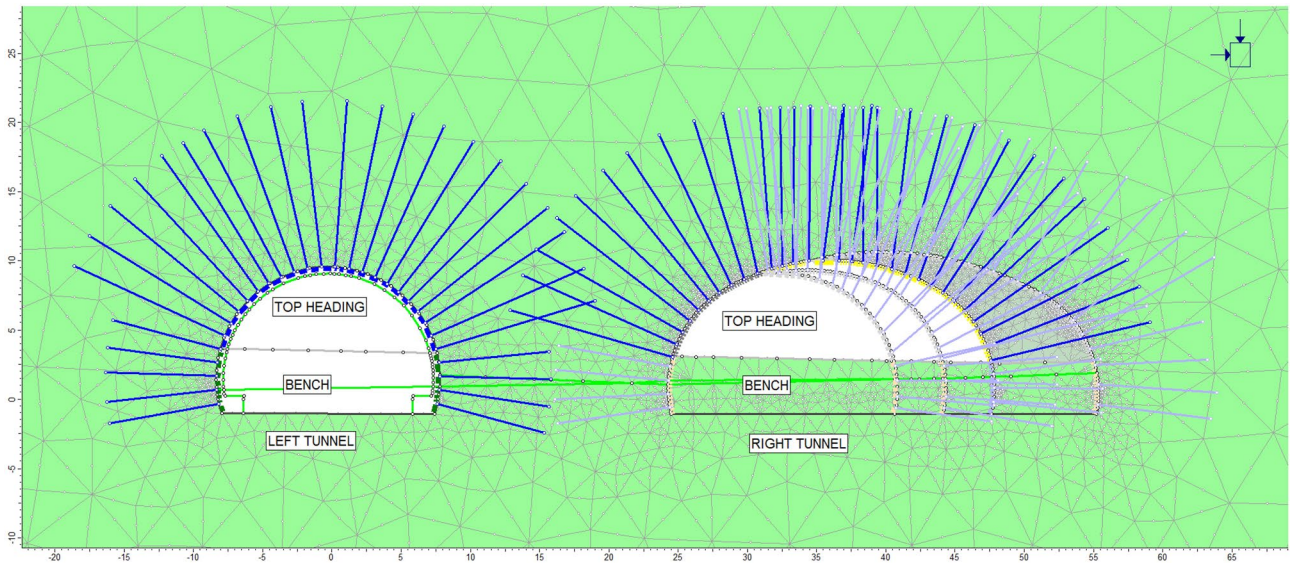


Fig. 21 Expansion section of right tunnel; stage 12, installation of tunnel support systems

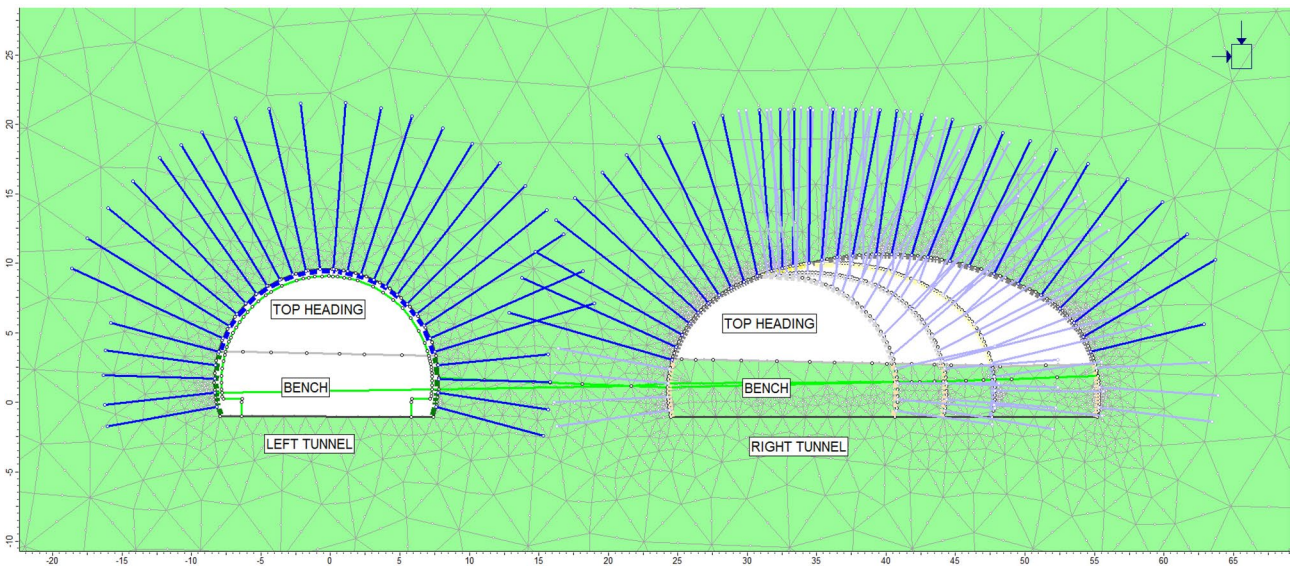


Fig. 22 Top heading section of right tunnel; stage 13, installation of tunnel support systems

Table 7 Deformations developed regarding to excavation stages

Tunnel	Stage no	Excavation stages	Point 1	Point 2	Point 3	Point 4
			Deformation (mm)			
Left tunnel	1	Initial conditions	0	0	0	0
	2	Top heading excavation, material softening	0	0	0	0
	3	TH support installation	0	0	0	0
	4	Bench excavation, material softening	0	0	0	0
	5	Bench support installation	0	0	0	0
Right tunnel	6	Top heading excavation, material softening	0	0	0	0
	7	TH support installation	3.4	3	1.4	0.4
	8	TH enlargement 1 excavation	3.75	3.5	1.75	0.5
	9	TH enlargement 1 support installation	4	4.25	2.75	0.5
	10	TH enlargement 2 excavation	4.2	4.5	3	0.6
	11	TH enlargement 2 support installation	4.8	5.4	4.5	0.9
	12	TH enlargement 3 excavation	5.6	6.8	6	2.4
	13	TH enlargement 3 support installation	6	7.2	7.2	4.4
	14	TH enlargement 3 excavation	6	7	7	4.5
	15	Bench excavation, material softening	6	7	7.5	4.5
	16	Bench support installation	6.05	7.15	7.15	4.4
	17	Bench enlargement 1 excavation	6	7.5	7.5	4.5
	18	Bench enlargement 1 support installation	6.05	7.15	7.15	4.4
	19	Bench enlargement 2 excavation	6.3	7.2	7.2	4.5
	20	Bench enlargement 2 support installation	6.07	7.5	7.5	5
	21	Bench enlargement 3 excavation	6	7.2	7.8	4.8
	22	Bench enlargement 3 support installation	7	8.4	8.4	6.3
	23	All support shotcrete hard	7	8.4	8.4	6.3
	24	Seismic loading	7	8.4	8.4	6.3

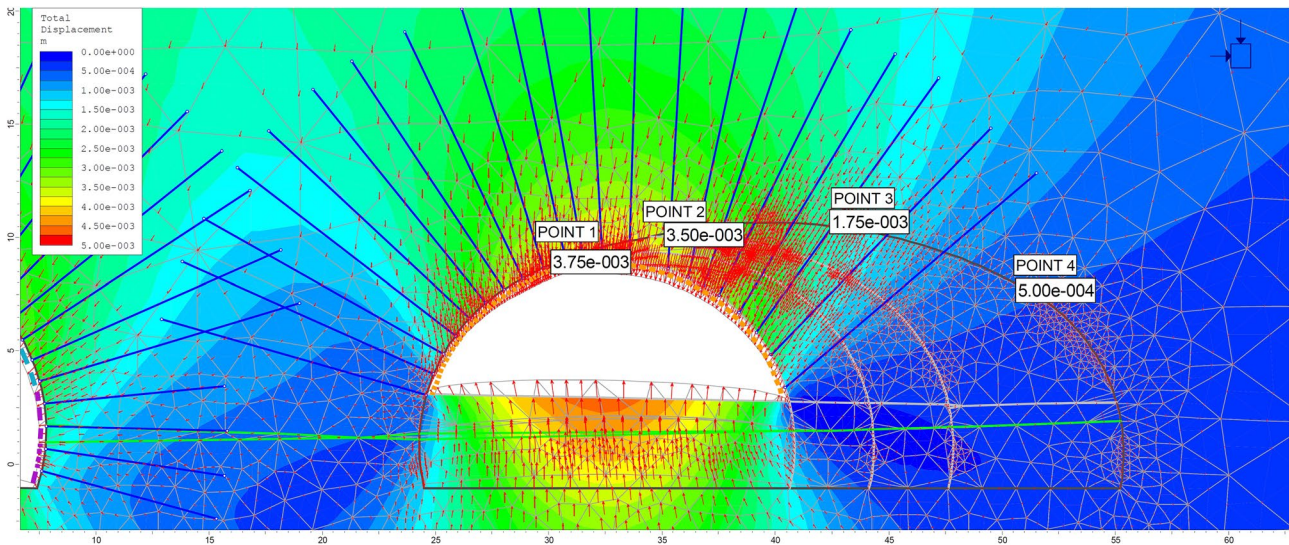


Fig. 23 Total deformations, stage 7 in Table 6

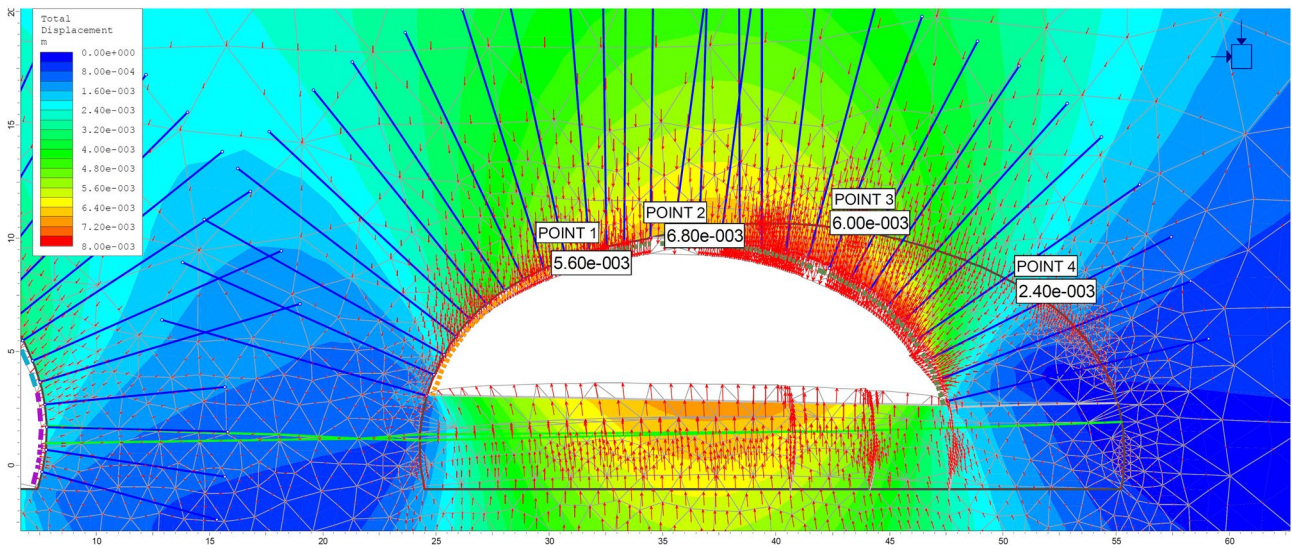


Fig. 24 Total deformations, stage 12 in Table 6

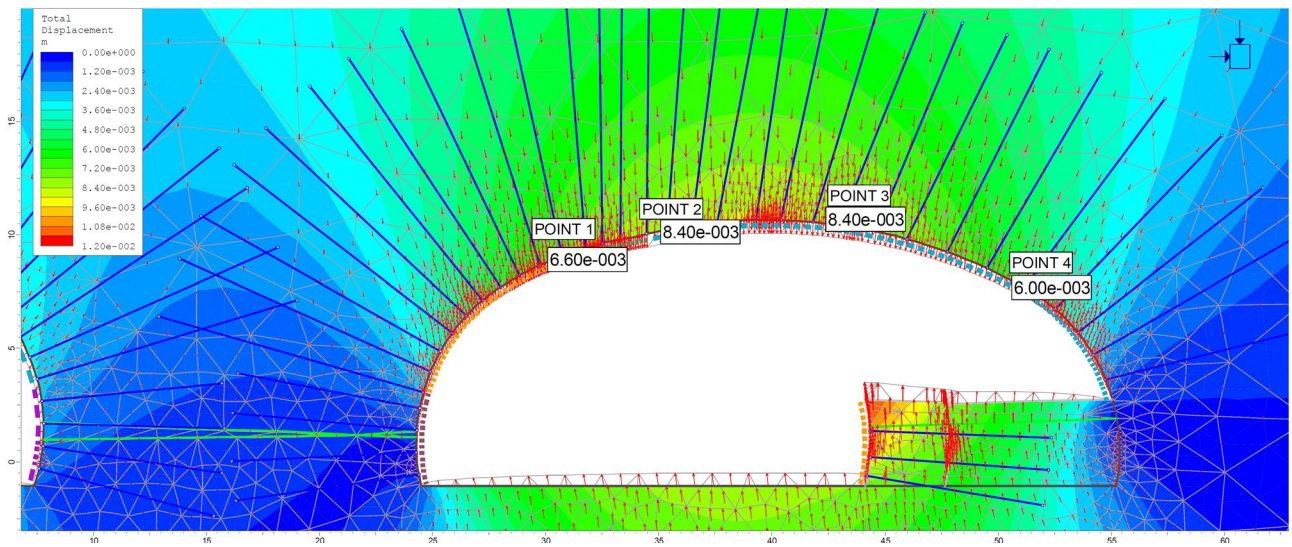


Fig. 25 Total deformations, stage 17 in Table 6

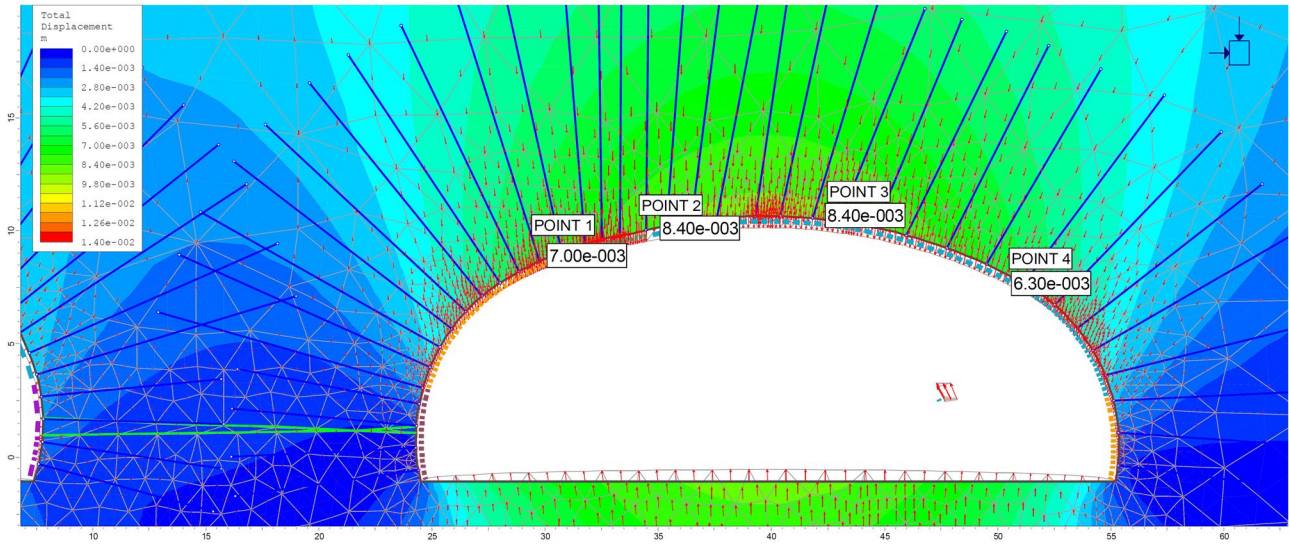


Fig. 26 Total deformations, stage 22 in Table 6

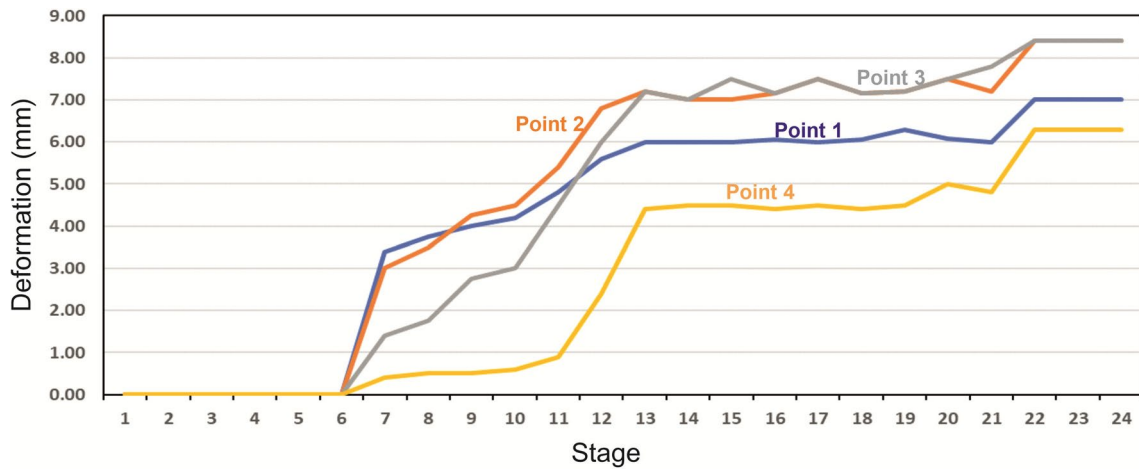


Fig. 27 Deformations obtained from the numerical analyses

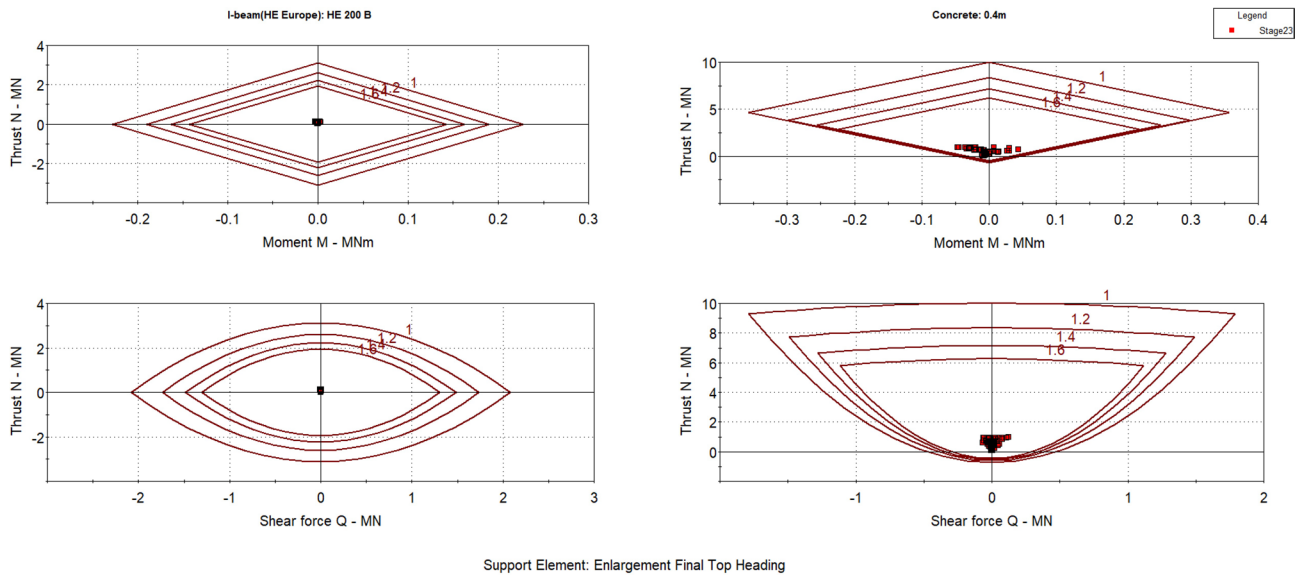


Fig. 28 Support capacity plots

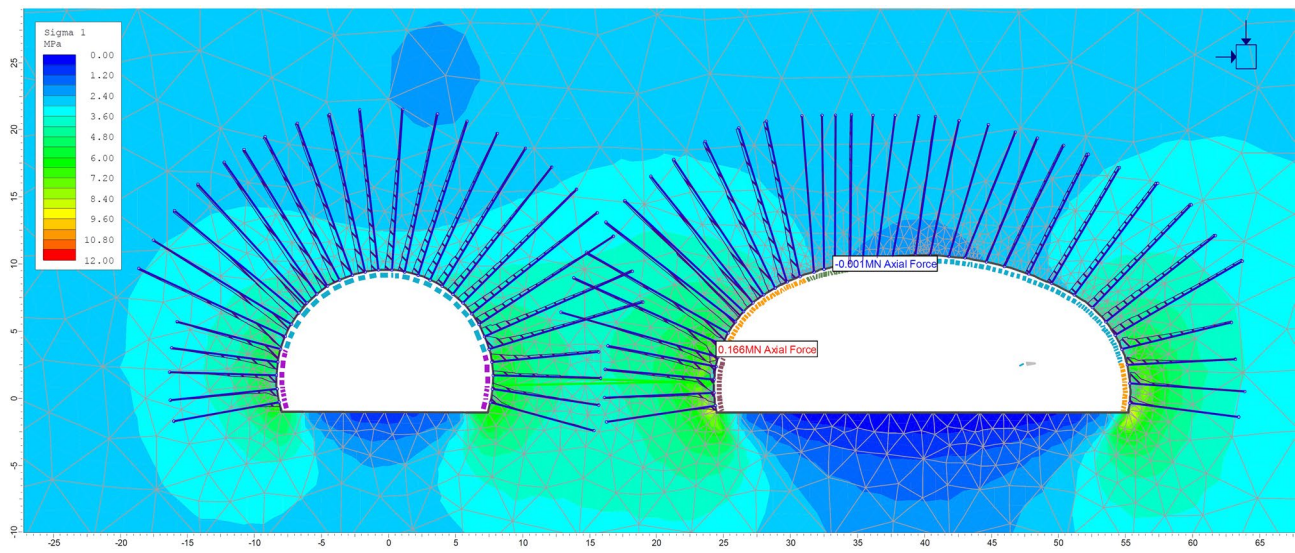


Fig. 29 Axial force at bolts for second case

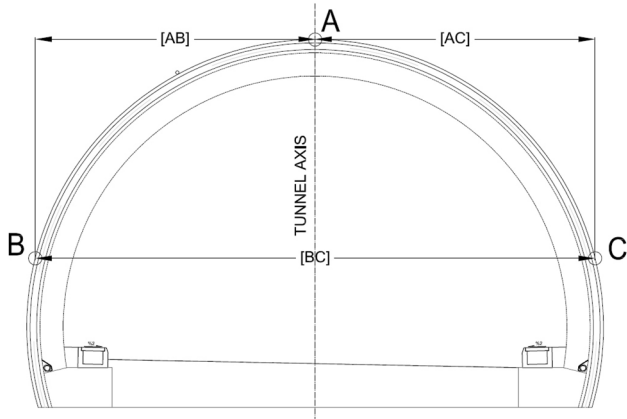


Fig. 30 Deformation measurement points

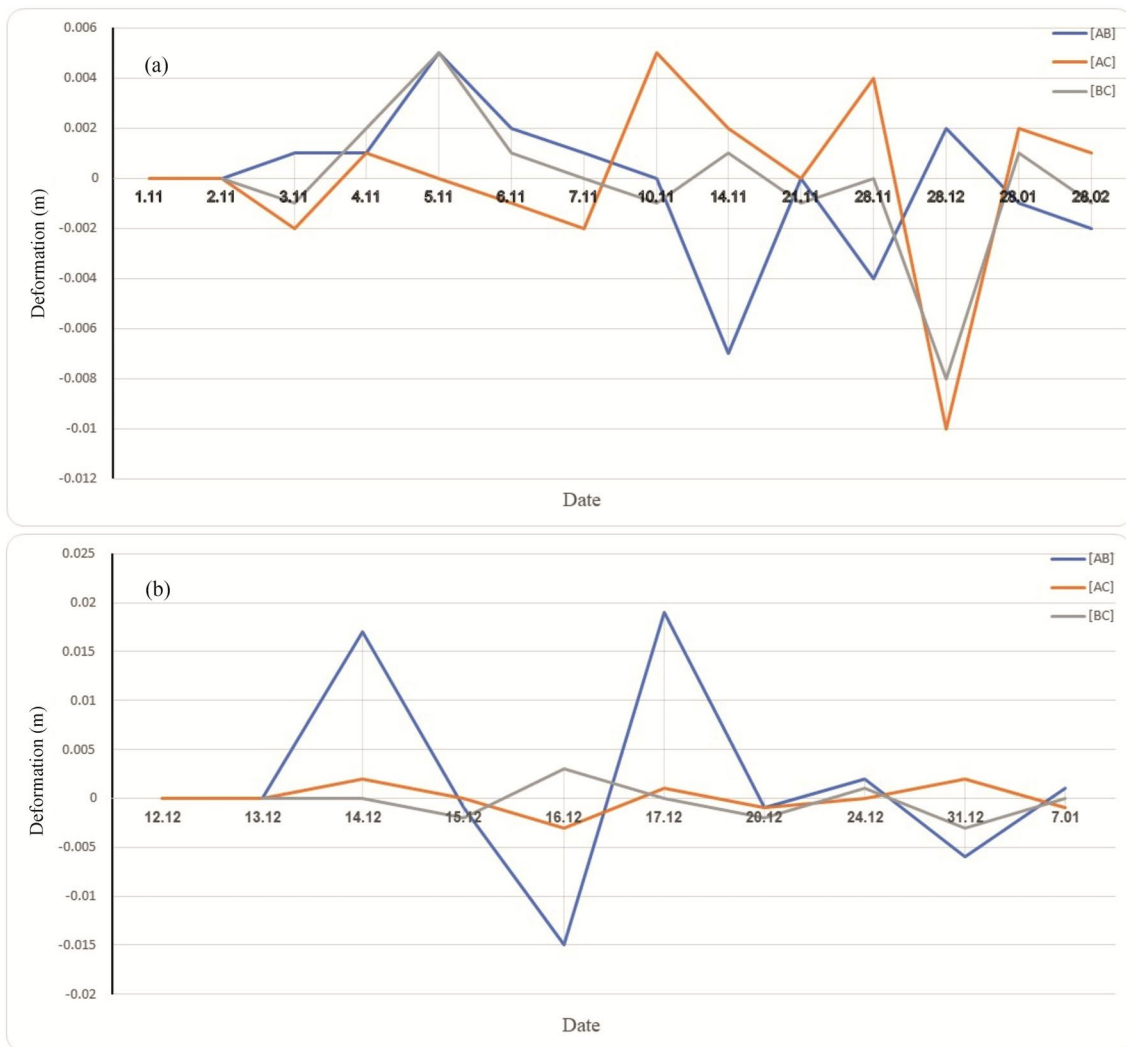


Fig. 31 Deformations at **a** Km:2 + 544.00 and **b** Km:2 + 569.00

Fig. 32 Excavation profile of Akyazı tunnel expansion zone [20]

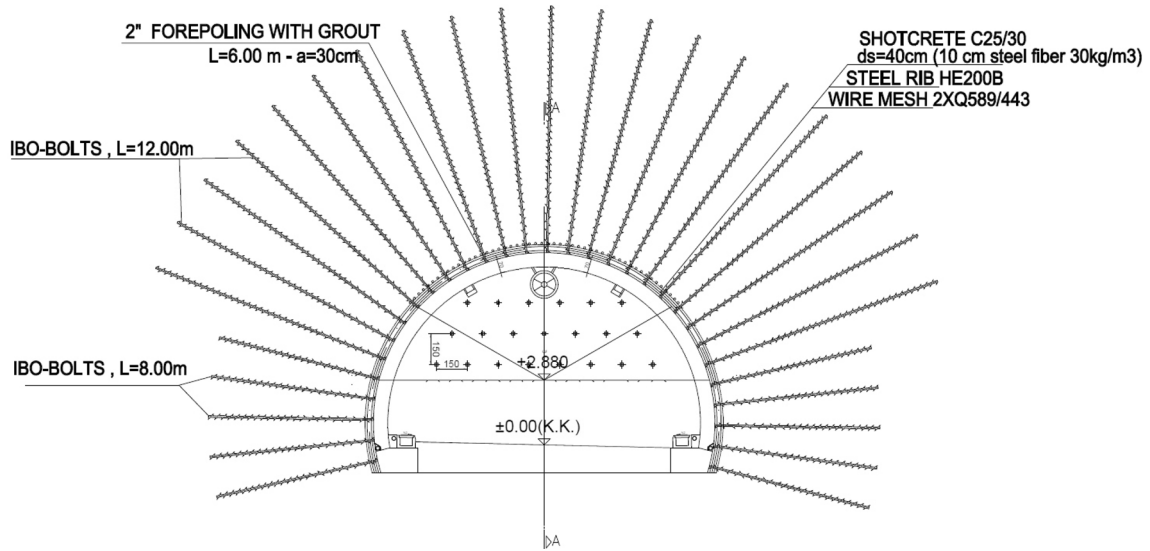
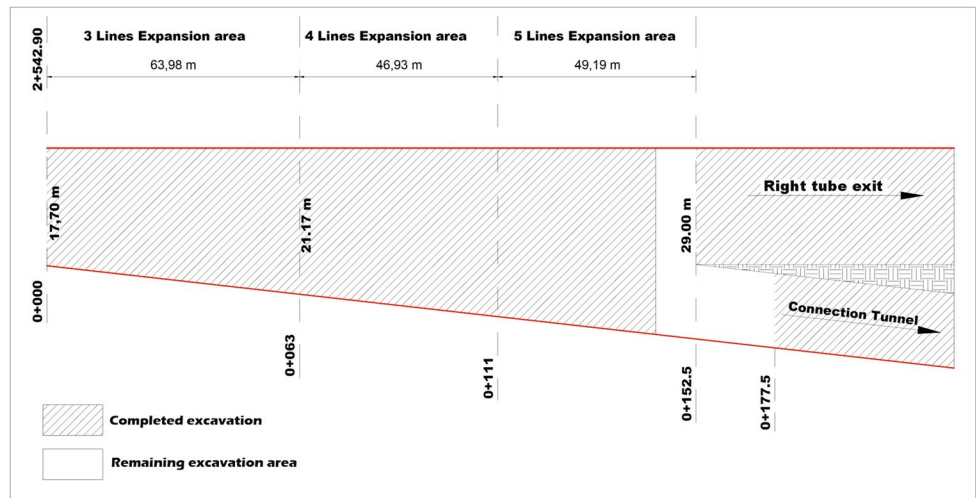


Fig. 33 Details of tunnel support class between Km:0+000-0+063.9 [20]

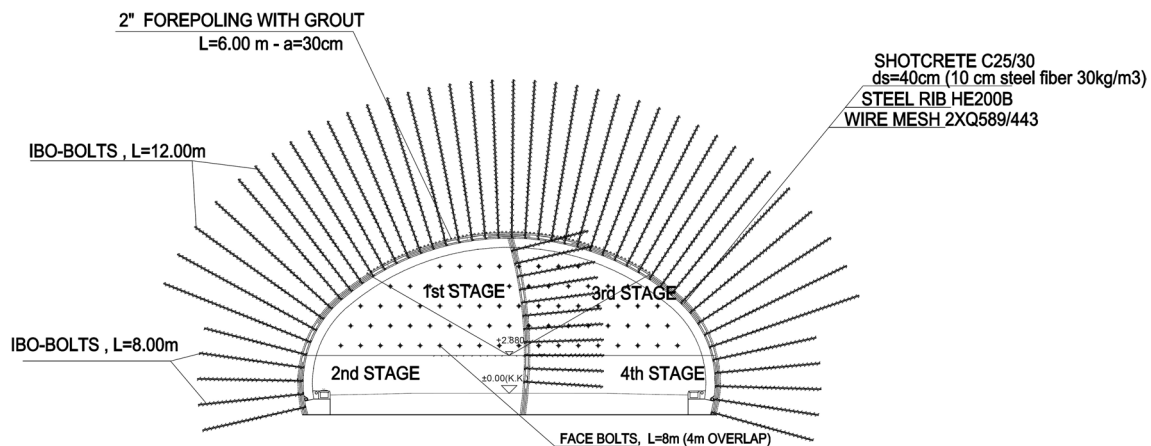


Fig. 34 Details of tunnel support class between Km:0 + 063.98-0 + 174.90 [20]

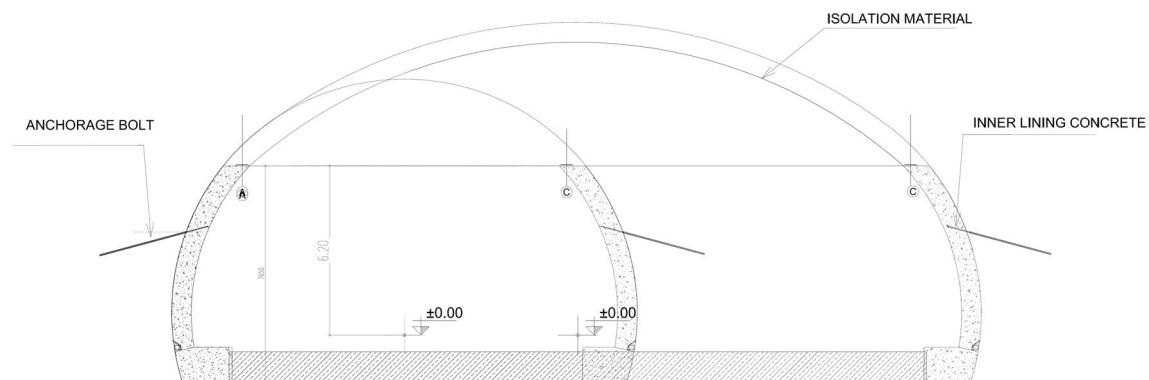


Fig. 35 Inner lining section with isolation material

projects and minimize uncertainties during excavation and installation of support systems and ensure successful completion of tunnel construction. This study provides promising results for economical and special inner lining design.

Acknowledgments The authors thank to General Directorate of KGM (General Directorate of Highways) and Fugro Sial Co for their supports.

Compliance with ethical standards

Conflict of interest The authors have no conflicts of interest to declare that are relevant to the content of this article.

Open Access This article is licensed under a Creative Commons Attribution 4.0 International License, which permits use, sharing, adaptation, distribution and reproduction in any medium or format, as long as you give appropriate credit to the original author(s) and the source, provide a link to the Creative Commons licence, and indicate if changes were made. The images or other third party material in this

article are included in the article's Creative Commons licence, unless indicated otherwise in a credit line to the material. If material is not included in the article's Creative Commons licence and your intended use is not permitted by statutory regulation or exceeds the permitted use, you will need to obtain permission directly from the copyright holder. To view a copy of this licence, visit <http://creativecommons.org/licenses/by/4.0/>.

References

1. Hoek E (2001) Big tunnels in bad rock 2000 terzaghi lecture. *ASCE J Geotechnical Geoenviron Eng* 127(9):726–740
2. Hoek E (2012) Alternative ground control strategies in underground construction, practices and trends for financing and contracting tunnels and underground works
3. Hoek E, Guevara R (2009) Overcoming squeezing in the Yacambú-Quibor tunnel. *Venezuela Rock Mech Rock Eng* 42(2):389–418
4. Barla G (2016) Full-face excavation of large tunnels in difficult conditions. *J Rock Mech Geotech Eng* 8(3):294–303

5. Sharifzadeh M, Kolivand F, Ghorbani M, Yasrobi S (2013) Design of sequential excavation method for large span urban tunnels in soft ground- the case of Niayesh road tunnel Project. *Tunn Undergr Space Technol* 35:178–188
6. Jiao JP, Wen Z, Xi D, Yang C, Chaozhe Z, Qian B, Zhiguo W (2019) Study on ground settlement and structural deformation for large span subway station using a new pre-supporting system. *R Soc Open Sci* 6:181035. <https://doi.org/10.1098/rsos.181035>
7. Hoek E (2007) Practical rock engineering, *Rock Science*, 341p
8. Schubert W (1996) Dealing with squeezing conditions in Alpine tunnels. *Rock Mech Rock Eng* 29(3):145–153
9. Aygar EB, Gokceoglu C (2020) Problems encountered during a railway tunnel excavation in squeezing and swelling materials and possible engineering measures: a case study from Turkey. *Sustainability* 12(3):1166. <https://doi.org/10.3390/su12031166>
10. Azizi F, Koopialipour M, Khoshrou H (2018) Estimation of rock mass squeezing potential in tunnel route (case study: Kerman water conveyance tunnel). *Geotech Geol Eng*. 37:1671–1685. <https://doi.org/10.1007/s10706-018-0714-5>
11. Fuente M, Sulem J, Taherzadeh R, Subrin D (2020) Tunneling in squeezing ground: effect of the excavation method. *Rock Mech Rock Eng* 53:601–623
12. Liu W, Chen J, Chen L, Luo Y, Shi Z, Wu Y (2020) Nonlinear deformation behaviors and a new approach for the classification and prediction of large deformation in tunnel construction stage: a case study. *European J Environ Civil Eng*. <https://doi.org/10.1080/19648189.2020.1744482>
13. Aygar E (2000). A critical approach to the New Austrian tunneling method in Bolu Tunnels. MSc Thesis, Hacettepe University, The Department of Mining Engineering, Ankara, p 276
14. Aygar E 2007. Investigation of the Bolu Tunnel stability by means of static and dynamic analyses. PhD Thesis, Hacettepe University, The Department of Mining Engineering, Ankara, p 273
15. Broch E, Grøv E, Davik KI (2002) The inner lining system in Norwegian traffic tunnels. *Tunn Undergr Space Technol* 17(3):305–314
16. Galler R, Lorenz S (2018) Support elements in conventional tunneling – Focus on long-term behavior. *Undergr Space* 3:277–287
17. Grønhaug A (1999) Lining designs for Norwegian road tunnels. In: Alten A et al (eds) *Challenges for the 21 st Century*. Balkema, Rotterdam, pp 347–352
18. Neuner M, Dummer A, Schreter M, Hofstetter G, Cordes T, Bergmeister K (2020) Nonlinear time-dependent analysis of the load-bearing capacity of a single permanent shotcrete lining at the brenner base tunnel. *Struct Eng Int* 30(4):475–483. <https://doi.org/10.1080/10168664.2020.1735979>
19. Ak H, Aksoy M (2017) Akyazi tüneli patlatmalı kazı çalışmalarında oluşan titreşimlerin çevresel etkilerinin araştırılması. *Yer Altı Kaynakları Dergisi* 13:1–12 ((in Turkish))
20. Fugro Sial Geosciences Consulting and Engineering (2012a) Akyazi Tunnel Project Report. Fugro Sial Co. (unpublished, in Turkish), 384p
21. Güven IH (1993) 1/25000 Scaled Geological and metallogenic map of East Blacksea Region. Publication of General Directorate of Mineral Research and Exploration, Ankara (Unpublished, in Turkish), 165p
22. Fugro Sial Geosciences Consulting and Engineering (2012b) Akyazi Tunnel Geological and Geotechnical Investigation Report. Fugro Sial Co.(unpublished, in Turkish), 193p
23. Hoek E, Brown ET (1997) Practical estimates of rock mass strength. *Int J Rock Mech Min Sci* 34(8):1165–1186
24. Hoek E, Marinos P (2000) Predicting tunnel squeezing. *Tunnels and tunnelling international*. Part 1–November 2000, Part 2–December 2000
25. General Directorate of Highways (KGM) (2014) Araştırma Mühendislik Hizmetleri Teknik Şartnamesi. T.A.D.B, Teknik Araştırma Dairesi Başkanlığı
26. Hashash YMA, Hook JJ, Schmidt B, Yao JI-C (2001) Seismic design and analysis of underground structures, ITA/AITES Accredited Material. *Tunn Undergr Sp Technol* 16:247–293
27. Federal Highway Administration (2009) Technical manual for design and construction of road tunnels-Civil Elements, p 702
28. Vlachopoulos N, Diederichs MS (2009) Improved longitudinal displacement profiles for convergence confinement analysis of deep tunnels. *Rock Mech Rock Eng* 42(2):131–146
29. Sheorey PR (1994) A theory for in situ stresses in isotropic and transversely isotropic rock. *Int J Rock Mech Min Sci Geomech Abstr*. 31(1):23–34
30. Lunardi P (2008) Design and construction of tunnels, analysis of controlled deformation in rocks and soils (ADECO_RS). Springer, Berlin Heidelberg, p 587
31. Duffaut P (2011) Large caverns, design and construction, 12th ISRM Congress, Beijing, China, Paper I-3

Publisher's Note Springer Nature remains neutral with regard to jurisdictional claims in published maps and institutional affiliations.